AD-A187 239 EFFECTS OF ION IMPLANTATION ON CAVITATION EROSION OF A COBALT BASED METAL..(U) WORCESTER POLYTECHNIC INST MA DEPT OF MECHANICAL ENGINEERING.. S A DILLICH SEP 87 1/1

UNCLASSIFIED N00014-86-K-0391 F/G 11/6.1 NL

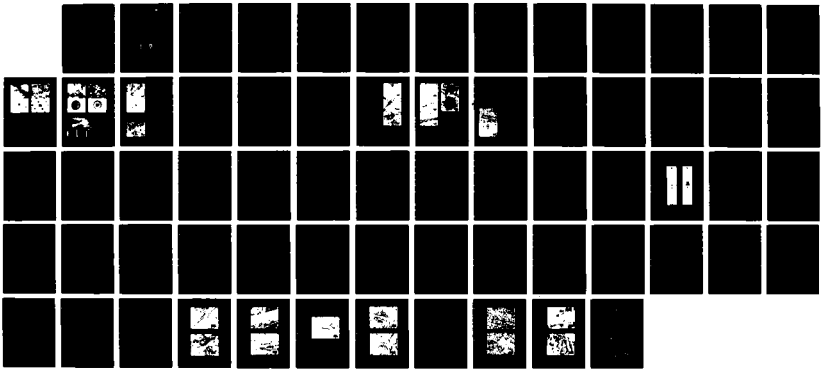

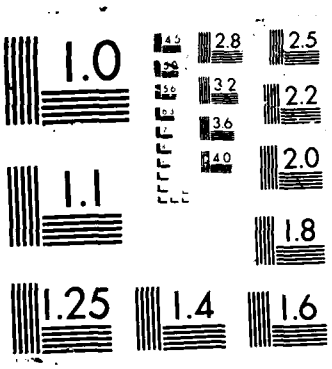
1.0
2.8
2.5
3.2
2.2
3.6
4.0
2.0
1.1
1.8
1.25
1.4
1.6

(2)

DTIC FILE COPY

Reports in Materials Science and Engineering

AD-A187 239

EFFECTS OF ION IMPLANTATION ON
CAVITATION EROSION OF A COBALT BASED
METAL/CARBIDE ALLOY

Submitted by:

Sara A. Dillich
Department of Mechanical Engineering
Worcester Polytechnic Institute
Worcester, Mass. 01609

DTIC
ELECTE
OCT 2 0 1987
S D
D

Mechanical Engineering Department
Worcester Polytechnic Institute
Worcester, Massachusetts 01609

DISTRIBUTION STATEMENT A
Approved for public release;
Distribution Unlimited

87 10 9 035

2

Final Report
Contract No. N00014-86-K-0391

EFFECTS OF ION IMPLANTATION ON CAVITATION EROSION OF A COBALT BASED METAL/CARBIDE ALLOY

Submitted by:

Sara A. Dillich
Department of Mechanical Engineering
Worcester Polytechnic Institute
Worcester, Mass. 01609

Submitted to:

Office of Naval Research
Materials Division, Code 1131M
800 N. Quincy Street
Arlington, Va. 22217

S
D

September, 1987

Approved for public release, distribution unlimited.
Reproduction in whole or in part is permitted for any purpose of the United States Government.

unclassified

SECURITY CLASSIFICATION OF THIS PAGE

REPORT DOCUMENTATION PAGE

1a. REPORT SECURITY CLASSIFICATION unclassified	1b. RESTRICTIVE MARKINGS
2a. SECURITY CLASSIFICATION AUTHORITY	3. DISTRIBUTION / AVAILABILITY OF REPORT unlimited
2b. DECLASSIFICATION / DOWNGRADING SCHEDULE	
4. PERFORMING ORGANIZATION REPORT NUMBER(S) Final Report 1987	5. MONITORING ORGANIZATION REPORT NUMBER(S)
6a. NAME OF PERFORMING ORGANIZATION Worcester Polytechnic Institute 6b. OFFICE SYMBOL (If applicable)	7a. NAME OF MONITORING ORGANIZATION Office of Naval Research
6c. ADDRESS (City, State, and ZIP Code) Dept. of Mechanical Engineering Worcester, Mass. 01609	7b. ADDRESS (City, State, and ZIP Code) Materials Division, Code 1131 M 800 N. Quincy Street Arlington, Va. 22217
8a. NAME OF FUNDING / SPONSORING ORGANIZATION Office of Naval Research 8b. OFFICE SYMBOL (If applicable)	9. PROCUREMENT INSTRUMENT IDENTIFICATION NUMBER N00014-86-K-0391
8c. ADDRESS (City, State, and ZIP Code)	10. SOURCE OF FUNDING NUMBERS

PROGRAM ELEMENT NO	PROJECT NO	TASK NO	WORK UNIT ACCESSION NO
61153N22	4323	4323	4323053

11. TITLE (Include Security Classification)

Effects of Ion Implantation on Cavitation Erosion of a Cobalt Based Metal/Carbide Alloy

12. PERSONAL AUTHOR(S) Sara A. Dillich

13a. TYPE OF REPORT	13b. TIME COVERED	14. DATE OF REPORT (Year, Month, Day)	15. PAGE COUNT
Final	FROM 6/1/86 TO 8/30/87	1987, September	64

16. SUPPLEMENTARY NOTATION

17. COSATI CODES			18. SUBJECT TERMS (Continue on reverse if necessary and identify by block number)
FIELD	GROUP	SUB-GROUP	
11-06-01	11-08	13-09	cavitation erosion, ion implantation, wear, carbides

19. ABSTRACT (Continue on reverse if necessary and identify by block number)

The goal of this work was to characterize the cavitation erosion wear mechanisms in a cobalt based superalloy and to investigate how these could be altered by high fluence titanium and nitrogen implantations. Both Ti and N implantations significantly improved the cavitation erosion resistance of the alloy, primarily through implantation effects in the cobalt rich matrix phase.

The Ti implanted samples showed the highest erosion resistances, as a result of the microstructural changes produced in the alloy during implantation. Namely, a carburized surface layer was formed, with an amorphous matrix phase and recrystallized carbides. A corresponding toughening of the matrix phase and decrease in the elastic modulus difference between matrix and carbide phases can account for the observed increased erosion resistance of this phase and enhanced carbide-matrix cohesion. Nitrogen implantation stabilized the metastable fcc matrix phase of the alloy (i.e., inhibited stress induced

20. DISTRIBUTION / AVAILABILITY OF ABSTRACT ☒ UNCLASSIFIED/UNLIMITED ☐ SAME AS RPT ☐ DTIC USERS	21. ABSTRACT SECURITY CLASSIFICATION unclassified
22a. NAME OF RESPONSIBLE INDIVIDUAL W. Ruff	22b. TELEPHONE (Include Area Code) (202) 696-4401 22c. OFFICE SYMBOL ONR Code 1131 M

DD FORM 1473, 84 MAR

83 APR edition may be used until exhausted
All other editions are obsolete

SECURITY CLASSIFICATION OF THIS PAGE

unclassified

19. ABSTRACT cont.

martensitic fcc to hcp transformations in the cobalt rich phase) with consequent prolonged matrix phase ductility and decreased carbide-matrix debonding during cavitation erosion. Similar improvements in erosion resistance as a result of increased durability of the cobalt rich binder phase were seen in 6%Co-WC cemented carbide samples implanted with Ti of N.

This report consists of four papers which cover the major findings and results of this research.

TABLE OF CONTENTS

ACKNOWLEDGEMENTS ii

FORWARD 1

INDEX OF TECHNICAL REPORTS 3

INDEX OF PUBLICATIONS 3

PUBLICATIONS: 4

"Structural Changes in a Cobalt-Based Alloy after High Fluence Ion Implantation", S. A. Dillich and R. R. Biederman

"Effects of Titanium Implantation on Cavitation Erosion of Cobalt-Based Metal-Carbide Systems", N. V. H. Gately and S. A. Dillich

"Effects of N Implantation on the Tribology and Microstructure of Cobalt Based Systems", N. V. H. Gately and S. A. Dillich

"X-Ray Diffraction Evaluation of the Effects of Nitrogen Implantation on Stress Induced Structural Changes in a Cobalt Based Alloy", N. V. H. Gately and S. A. Dillich

DTIC COPY INSPECTED 2

Accesion For
NTIS CRA&I
DTIC TAB
Unannounced
Justification
By
Distribution/
Availability Codes
Dist
A-1

ACKNOWLEDGMENTS

The financial support of this work by the Office of Naval Research, and the advice and encouragement of Dr. Peter Blau, are gratefully acknowledged.

The cavitation erosion tests were performed by Mr. Nicholas Gately, graduate research assistant, WPI. The cemented carbide samples used in this study were donated by the GTE Research Laboratories in Waltham, Mass. The implantations necessary for this work were performed at the Naval Research Laboratory, Washington D.C. by the Surface Modification and Materials Analysis Group, and at the GTE Research Laboratories.

FORWARD

In this work, cavitation erosion tests were performed on nonimplanted, Ti implanted (5×10^{17} Ti/cm^2, 190 keV) and N implanted (4×10^{17} N/cm^2, 50 keV) samples of a cobalt based superalloy (Stoody 3, Co-31Cr-12.5W-2.2C) and a 6%Co-WC cemented carbide. Cavitation tests were made using a vibrating horn geometry, in accordance with ASTM standard G32-85. Surface damage and material loss from the samples were monitored by periodic weight loss measurments and SEM examinations of the test surfaces. Transmission electron microscopy and X-ray diffraction examinations with a Read thin film camera as well as with a diffractometer were used to investigate microstructural changes occuring in the alloy as a result of implantation.

The intent of this research was to a) characterize the cavitation erosion wear mechanisms in cobalt based metal/carbide composite systems and b) investigate how these mechanisms could be altered by high fluence titanium and nitrogen ion implantations. Of particular interest was the determination of the contributions of individual metal matrix and carbide phases to the erosive wear of the nonimplanted and implanted materials. This report consists of four papers which cover the major findings and results of the research. A summary of these results is given below.

Erosion of the Stoody 3 alloy began with crack propagation through the carbides and debonding at the carbide-matrix interfaces, after which material loss from both matrix and carbide phases took place. Measureable weight loss coincided with the appearance of matrix phase damage. Both Ti and N implantations improved the erosion resistance of the alloy; primarily through implantation effects in the matrix phase which resulted in diminished matrix phase erosion and carbide-matrix debonding.

The erosion resistance of the alloy was most improved by Ti implantation. The outstanding erosion resistance of the Ti implanted alloy can be explained by the microstructural and chemical changes that occurred during implantation. Ti implantation of the alloy produced high surface compressive stresses, and a carburized surface layer with an amorphous matrix phase and recrystallized carbides. The durability of the matrix phase increased with implantation, possibly as a result of the toughness of the amorphous layer. Amorphization of the matrix phase and recrystallization of the carbides contributed to the improved erosion resistance, it is believed, by decreasing the

difference in elastic moduli between matrix and carbide phases, thereby enhancing carbide-matrix cohesion. The introduction of compressive stresses by Ti implantation may also have augmented the cavitation erosion resistance of the matrix by reducing the detrimental effects of high cycle fatigue.

N implantation stabilized the metastable fcc matrix phase in the alloy, thereby reducing the incidence of stress induced fcc to hcp martensitic transformations during wear. The increased retention of the softer, more ductile fcc phase on implanted surfaces decreased the cavitation erosion rate of the alloy due to prolonged matrix phase ductility and reduced debonding at carbide/matrix phase interfaces.

Erosion rates of the cemented carbide samples were an order of magnitude higher than those of the Stoody 3 samples, a result of the higher carbide/matrix interface density of these samples. Erosion of these samples was matrix phase dependent, i.e., rapid loss of the cobalt phase was followed by attrition rather that erosion of the carbide particles. Both N and Ti implantations improved the erosion resistance of the samples, with Ti implantation having the largest effect. Structural changes in the implanted cemented carbides were not determined. However, the effects of implantation appeared, as in the case of the Stoody 3 alloy, primarily in the cobalt rich binder phase. It is likely, then, that the improved erosion resistance of the implanted cemented carbides may by credited to the same mechanisms active in the implanted Stoody 3 alloy.

INDEX OF TECHNICAL REPORTS

End of Fiscal Year Report, submitted to ONR 9/86.

End of Fiscal Year Report, submitted to ONR 9/87.

Final Report, submitted to ONR 9/87.

INDEX OF PUBLICATIONS

"Structural Changes in a Cobalt-Based Alloy after High Fluence Ion Implantation", S. A. Dillich and R. R. Biederman, Materials Science and Engineering, 90, (1987), pp. 91 - 97.

"Effects of Titanium Implantation on Cavitation Erosion of Cobalt-based Metal-Carbide Systems", N. V. H. Gately and S. A. Dillich, Materials Science and Engineering, 90, (1987), pp. 333 - 338.

"Effects of N Implantation on the Tribology and Microstructure of Cobalt Based Systems", N. V. H. Gately and S. A. Dillich, submitted for publication to Surface and Coatings Technology.

"X-Ray Diffraction Evaluation of the Effects of Nitrogen Implantation on Stress Induced Structural Changes in a Cobalt Based Alloy", N. V. H. Gately and S. A. Dillich. To be published in V. 16 of Microstructural Science.

Master's Thesis:

"Effects of High Fluence Ion Implantation on the Cavitation Erosion Resistance of Cobalt Based Systems", N. V. H. Gately, WPI, 1987.

PUBLICATIONS

1. "Structural Changes in a Cobalt-Based Alloy after High Fluence Ion Implantation", S. A. Dillich and R. R. Biederman

2. "Effects of Titanium Implantation on Cavitation Erosion of Cobalt-Based Metal-Carbide Systems", N. V. H. Gately and S. A. Dillich

3. "Effects of N Implantation on the Tribology and Micro - structure of Cobalt Based Systems", N. V. H. Gately and S. A. Dillich

4. "X-Ray Diffraction Evaluation of the Effects of Nitrogen Implantation on Stress Induced Structural Changes in a Cobalt Based Alloy", N. V. H. Gately and S. A. Dillich

Materials Science and Engineering, *90* (1987) 91–97

Structural Changes in a Cobalt-based Alloy after High Fluence Ion Implantation*

S. A. DILLICH and R. R. BIEDERMAN

Worcester Polytechnic Institute, Worcester, MA 01609 (U.S.A.)

(Received July 10, 1986)

ABSTRACT

Structural changes in a cobalt-based alloy (Co-31Cr-12.5W-2.2C where the composition is in approximate weight per cent; Stoody 3) as a result of high fluence nitrogen or titanium ion implantations were investigated via transmission electron microscopy and selected area diffraction examinations of unimplanted and implanted foils. The alloy microstructure was found to consist of several morphologies of single-crystal carbides (Cr–Co–W solutions) in a cobalt-rich f.c.c. matrix phase of high planar defect density. Titanium implantation (5×10^{17} Ti^+ cm^{-2} at 190 keV) produced a surface layer with an amorphous matrix phase and recrystallized carbides, while nitrogen implantation (4×10^{17} N^+ cm^{-2} at 50 keV) greatly increased the planar fault density in the matrix phase. Previously reported effects of titanium and nitrogen implantations on the tribological behavior of the alloy are discussed in terms of the results of these investigations.

1. INTRODUCTION

Cobalt-based alloys are among the most wear-resistant materials commercially available. These alloys consist of hard chromium and tungsten carbides (most often M_7C_3 and M_6C) dispersed in softer, more ductile cobalt-rich solid solutions. Although Co–Cr–W solid solutions normally have h.c.p. structures at low temperatures, for most applications the alloys are designed to have the more ductile metastable f.c.c. phase. The superior abrasion and erosion resistance of these alloys is attributed to their low stacking fault energies which allow low temperature localized martensitic f.c.c.-to-h.c.p. transformations to occur with strain at an abraded or eroded surface [1–3]. Thus, it is believed, the ductile bulk alloys are protected by surfaces with high strain-hardening characteristics.

Ion implantations of a cobalt-based superalloy (Co–31Cr–12.5W–2.2C where the composition is in approximate weight per cent; commercial designation, Stoody 3) with titanium and nitrogen have been found to produce significant changes in the tribological behavior of the alloy, as observed during abrasive wear, dry sliding friction and cavitation erosion tests [4–6]. The abrasion resistances of nitrogen- and titanium-implanted samples relative to that of the unimplanted alloy can be seen in Fig. 1. Titanium implantation of the alloy created abrasion-resistant surfaces which have also exhibited improved cavitation erosion resistance [6] and a 50%–70% reduction in dry sliding friction [4, 5]. Scanning Auger microscope analysis of titanium-implanted surfaces revealed that a vacuum-carburized titanium layer was produced on the alloy in both matrix and carbide phases during implantation [4]. Similar vacuum-carburized (Fe–Ti–C) surfaces found on titanium-implanted steels have been shown to be amorphous [7–9]. However, the existence of disordered phases in titanium-implanted Stoody 3 surfaces remained to be determined.

In contrast, the abrasive wear resistance of the Stoody 3 alloy dropped to about one-half of the bulk value after nitrogen implantation (Fig. 1). Although friction and erosion of the alloy remained high after nitrogen implantation, changes in the wear mode during dry sliding [5] and cavitation erosion tests [10] were observed. Nitrogen stabilization of the metastable f.c.c. matrix phase, with a resultant decrease in surface work hardening during sliding and abrasion, was offered as a possible

*Paper presented at the International Conference on Surface Modification of Metals by Ion Beams, Kingston, Canada, July 7–11, 1986.

0025-5416/87/$3.50

© Elsevier Sequoia/Printed in The Netherlands

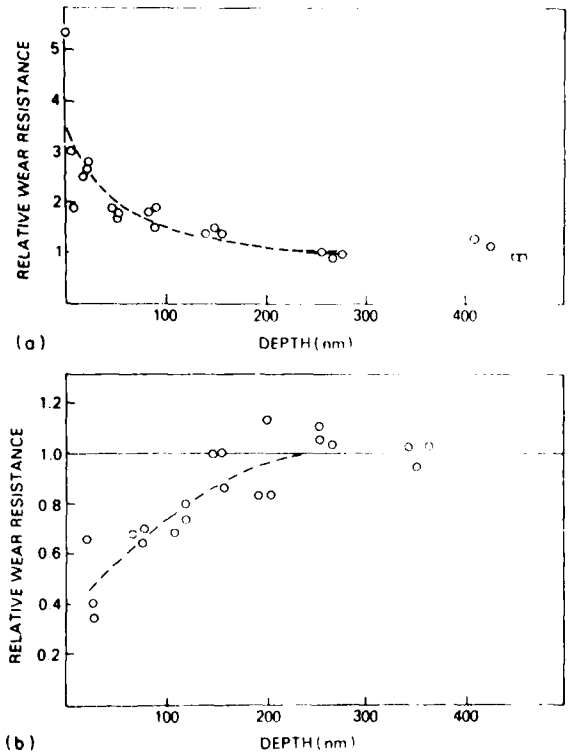

Fig. 1. Relative wear resistances of (a) titanium-implanted (5×10^{17} Ti^+ cm^{-2}; 190 keV) Stoody 3 samples and (b) nitrogen-implanted (4×10^{17} N^+ cm^{-2}; 50 keV) Stoody 3 samples, abraded with 1.5 μm diamond *vs.* depth [5]: ——, unimplanted Stoody 3 samples.

but unproven explanation of the observed behavior [5]. Since nitrogen has little or no solid solubility in cobalt, its effects as a phase stabilizer have not been documented. However, nitrogen stabilization of the f.c.c. phase in the binder alloy of a nitrogen-implanted cobalt-cemented tungsten carbide has been reported [11].

In this work, microstructural changes responsible for the observed tribological behavior of the titanium- and nitrogen-implanted alloy surfaces were investigated by transmission electron microscopy (TEM) and selected area diffraction (SAD) analyses of titanium-implanted, nitrogen-implanted and unimplanted alloy foils.

2. SAMPLE PREPARATION

TEM foils (3 mm in diameter) were punched from hand-ground disks (12.7 mm in diameter and 0.1 mm thick) and then polished on both sides to a 1 μm or less finish. Implant conditions for the foils were chosen to correspond to those used in the friction, wear and erosion studies discussed above, *i.e.* 5×10^{17} Ti^+ cm^{-2} at 190 keV or 4×10^{17} N^+ cm^{-2} at 50 keV. Implantations were performed in a modified model 200-20A2F Varion Extrion ion implanter with a hot-cathode arc discharge-type ion source. The samples were heat sunk onto a water-cooled holder during implantation to limit the temperature rise at the surfaces to less than 50 °C.

The foils were thinned by one-sided electropolishing at −50 °C, in a solution of 15% HNO in methanol. Plastic "dummy" foils protected the surface of interest (*i.e.* the implanted surface or for the unimplanted foils the as-polished surface) from the electrolyte during thinning.

3. RESULTS

Thinned regions on the foils were examined in a 100 kV JEOL 100C scanning transmission electron microscope. Transmission of electrons at this energy is limited to regions with a maximum thickness of about 150 nm, *i.e.* corresponding to the range of ion penetration on the implanted surfaces [5].

Microstructural features of the unimplanted material were first examined to establish a reference for the implanted surfaces. A scanning electron microscopy (SEM) micrograph of an unimplanted foil is shown in Fig. 2. Several distinct carbide morphologies can be distinguished in the alloy: large dark lath- or block-shaped carbides, a light "script" phase, and smaller light and dark elliptically shaped carbides dispersed between the larger carbides. Energy-dispersive X-ray analysis revealed the metal components of the carbides to be Cr Co W solutions, with the lighter carbides having higher tungsten concentrations than the darker carbides. Exact stoichiometries of these carbides have not yet been determined.

Bright field TEM micrographs and SAD patterns from unimplanted foils are shown in Figs. 3–5. The matrix phase of the alloy is characterized by networks of planar defects (predominantly stacking faults) running through the grains and extending occasionally from one matrix grain to another (Figs. 3 and

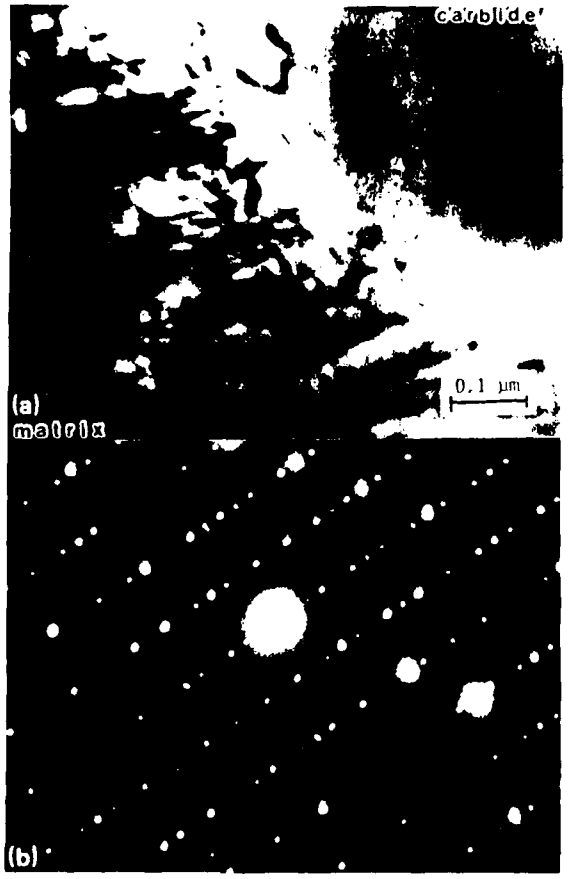

Fig. 5. (a) Bright field micrograph of a carbide matrix interface; (b) an SAD pattern from the carbide.

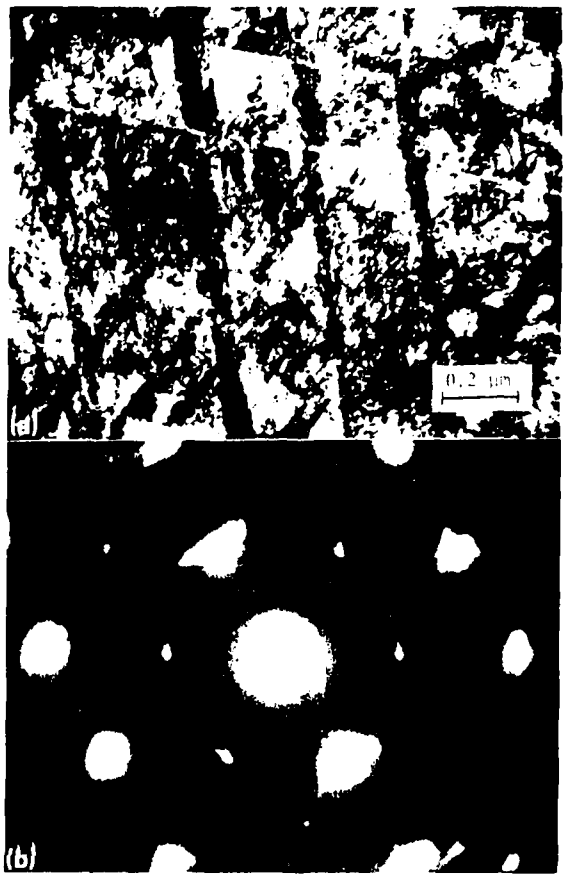

Fig. 6. (a) Bright field micrograph of the matrix phase in an unpolished foil; (b) the corresponding SAD pattern (211 zone; f.c.c.).

absence of defects, *i.e.* dislocations and planar faults (Fig. 7). Similarly, the carbides were transformed from monolithic single crystals to fine-grained polycrystals (Figs. 8 and 9), with diffraction spots forming ring patterns (Fig. 8). Partial amorphization of the carbide surfaces is suggested by the diffuse nature of the rings.

The carbides were outlined by borders of light contrast matrix material which, on close inspection, appeared to be carbide depleted. Energy-dispersive X-ray analysis of the border region shown in Fig. 9 indicated higher titanium concentrations in the carbides and bordering matrix than in the neighboring darker contrast matrix material. Preferential carburization (*i.e.* the formation of a titanium-plus-carbon-enriched surface layer [5]) at or near the carbides during implantation is a possible explanation of this result.

Micrographs from a nitrogen-implanted foil can be seen in Figs. 10 and 11. Single-crystal SAD patterns were obtained from both matrix and carbide phases on the foil. As was the case for the unimplanted foils, the matrix phase was found to be cubic (Fig. 10). Although nitrogen implantation did not produce changes in the crystallinity of the surface, a striking increase in the fault density was observed (compare Figs. 10 and 11 with Figs. 3 and 4).

4. DISCUSSION

In a previous work, it was found that titanium implantation modifies the chemistry of the Stoody 3 surface via vacuum carburization, *i.e.* the introduction of excess carbon atoms into the surface during implantation [4]. The TEM investigations described above revealed that microstructural changes (most notably a noncrystalline matrix phase) are

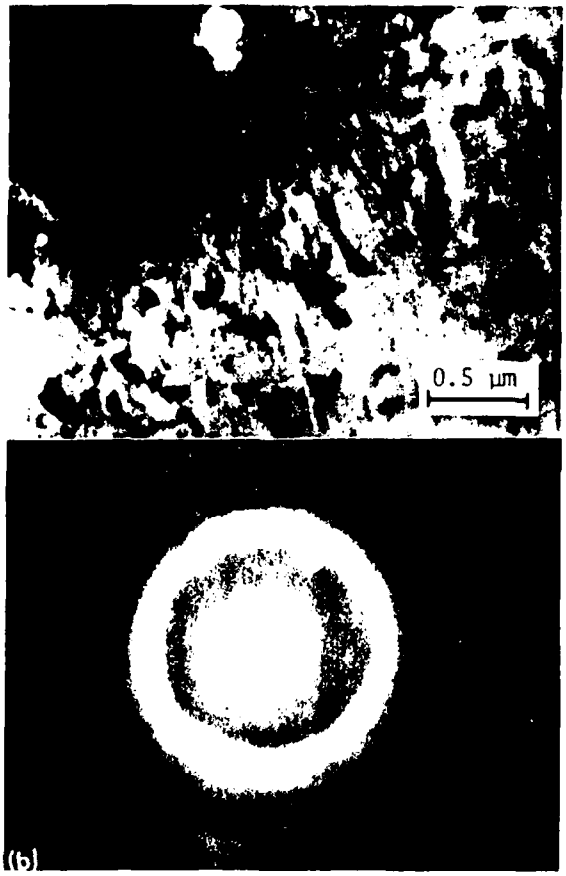

Fig. 7. (a) Bright field micrograph of the matrix phase in a titanium-implanted foil; (b) the corresponding SAD pattern.

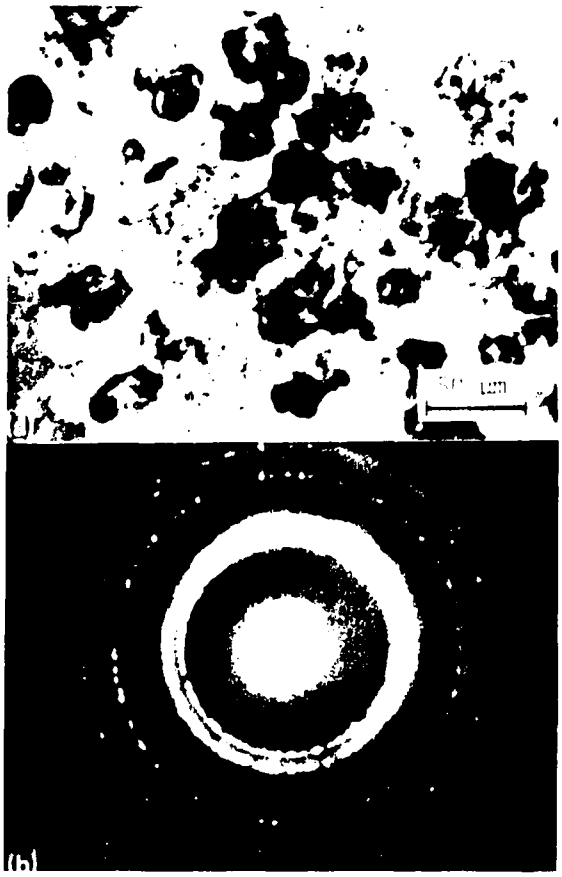

Fig. 8. (a) Bright field micrograph of a carbide in the titanium-implanted foil; (b) the corresponding SAD pattern. The rings in the pattern indicated a polycrystalline phase. Partial amorphization of the carbide surface is suggested by the diffuse nature of the rings.

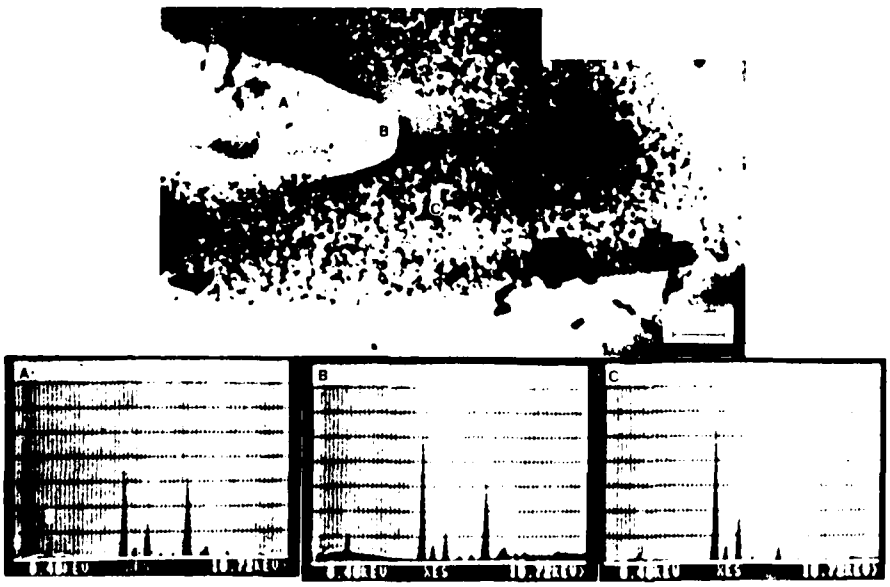

Fig. 9. Bright field micrograph of the titanium-implanted foil and energy dispersive X-ray spectra from (a) the matrix, (b) the matrix material bordering the carbide and (c) the carbide. The matrix appeared to have a lower surface concentration of titanium than the carbide or bordering matrix material does.

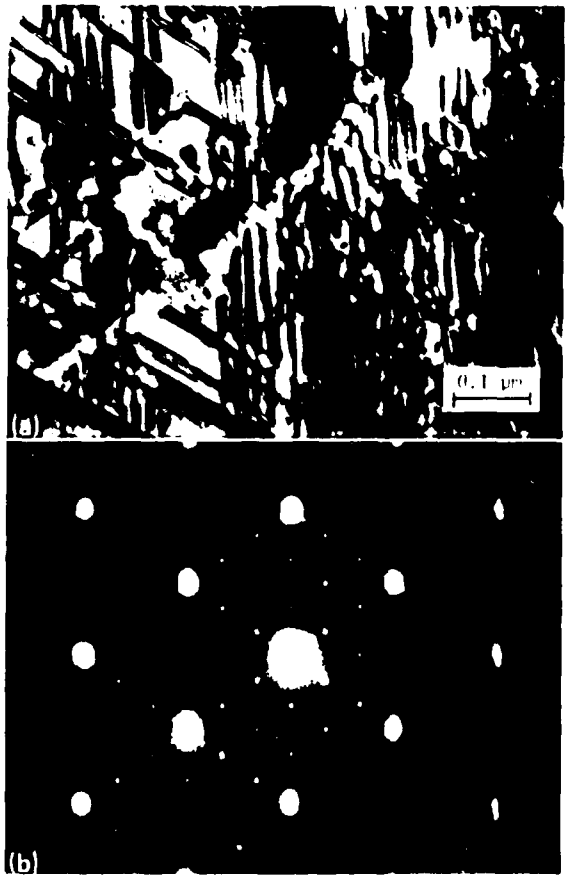

Fig. 10. (a) Bright field micrograph of the matrix phase in a nitrogen-implanted foil; (b) the corresponding SAD pattern (110 zone; f.c.c.). The extra spots grouped in clusters around the basic f.c.c. cobalt spots are believed to originate from carbides dispersed in the matrix.

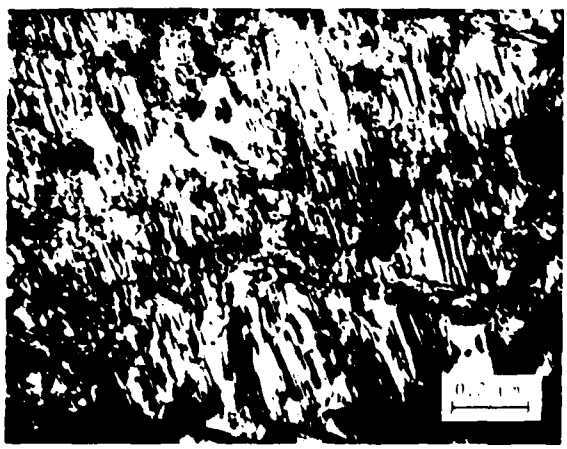

Fig. 11. Bright field micrograph of matrix regions in a nitrogen-implanted foil. Very high stacking fault densities were seen in this phase.

also produced, the result presumably of ion bombardment damage to the original crystalline lattice. This amorphous carburized layer provides a low friction wear-resistant alloy surface, as shown by dry sliding friction, abrasion and cavitation erosion tests.

SEM examinations of cavitation-eroded Stoody 3 surfaces have shown that the titanium implant layer inhibits debonding at carbide matrix interfaces and contributes additional toughness to the cobalt-based matrix, thereby delaying the loss of matrix phase material from the surface [6]. A corresponding increase in wear resistance of the carbides was not indicated, a consequence perhaps of recrystallization softening during implantation. This is consistent with results of other studies in which high fluence ion implantation has been found to cause softening [11, 12] and loss of wear resistance [13] in ceramic and carbide materials.

The superior wear resistance of the titanium-implanted Stoody alloy surfaces can, it appears, be attributed primarily to the matrix phase implant layer. However, the enhanced cohesion at carbide matrix interfaces observed on eroded titanium-implanted surfaces suggests that these regions also play an important role in determining alloy erosion and abrasion resistance. Further study is needed to characterize fully the chemistry and structure of the interface regions and their influence on the early stages of wear.

No attempt was made in this study to determine the minimum titanium ion fluence or energy necessary to drive the surface amorphous or to correlate improved tribological behavior with a critical surface concentration of carbon, nor has the role of carbon in the stabilization of the disordered phase been identified. These topics remain to be addressed in more extensive studies.

After nitrogen implantation the dominant microstructural change observed in the alloy was the extremely high stacking fault density in the matrix phase. The origin of this particular feature, *i.e.* whether it is due to implantation-induced damage or to the presence of nitrogen in the alloy lattice, or to both, is unclear. Also a complete explanation of the effects of nitrogen on the alloy tribology is not yet available. Since the metastable f.c.c. phase was found in both unimplanted and nitrogen-implanted alloy foils, the possible

role of nitrogen as an f.c.c. phase stabilizer cannot be commented on. It is possible that the presence of a greatly increased fault density in the implant layer limited the ability of the alloy to respond plastically under stress and that this effect, in and by itself, produced the poor abrasion resistance exhibited by the nitrogen-implanted Stoody 3 surfaces.

5. SUMMARY

TEM studies made on unimplanted and implanted foils revealed the microstructural changes resulting from titanium and nitrogen implantations. Amorphization of the cobalt-based matrix phase of the alloy after titanium implantation produces a low friction wear-resistant surface. Although nitrogen implantation does not alter the crystallinity of the alloy, a greatly increased stacking fault density is produced in the implant layer which results in a high friction, low wear resistance surface.

ACKNOWLEDGMENTS

We thank the Surface Modification and Materials Analysis Group, Naval Research Laboratory, Washington, DC, for their co-operation with implantations and James Steele (University of Connecticut) for the use of his diffraction pattern analysis software.

This work was supported through the materials division of the Office of Naval Research.

REFERENCES

1 K. C. Antony, *J. Met.*, *25* (February 1973) 52.
2 K. J. Bhansali and A. E. Miller, *Wear*, *75* (1982) 241.
3 C. J. Heathcock, A. Ball and B. E. Protheroe, *Wear*, *74* (1981–1982) 254.
4 S. A. Dillich and I. L. Singer, *Thin Solid Films*, *73* (1981) 219.
5 S. A. Dillich, R. N. Bolster and I. L. Singer, in G. K. Hubler, O. W. Holland, C. R. Clayton and C. W. White (eds.), *Ion Implantation and Ion Beam Processing of Materials, Materials Research Society Symp. Proc., Boston, MA, November 14–17, 1983*, Vol. 27, Elsevier, New York, 1984, p. 637.
6 N. V. H. Gately and S. A. Dillich, *Proc. Int. Conf. on Surface Modification of Metals by Ion Beams, Kingston, July 7–11, 1986*, in *Mater. Sci. Eng.*, *90* (1987).
7 I. L. Singer, C. A. Carosella and J. R. Reed, *Nucl. Instrum. Methods*, *182–183* (1981) 923.
8 D. M. Follstaedt, F. G. Yost and L. E. Pope, in G. K. Hubler, O. W. Holland, C. R. Clayton and C. W. White (eds.), *Ion Implantation and Ion Beam Processing of Materials, Materials Research Society Symp. Proc., Boston, MA, November 14–17, 1983*, Vol. 27, Elsevier, New York, 1984, p. 661.
9 J. A. Knapp, D. M. Follstaedt and B. L. Doyle, *Nucl. Instrum. Methods B*, *7–8* (1985) 38.
10 N. V. H. Gately and S. A. Dillich, unpublished work, 1987.
11 G. Dearnaley, B. James, D. J. Mazey and F. J. Minter, *Proc. Plansee Conf., 1985*, Metallwerk Plansee, Reutte, in the press.
12 P. J. Burnett and T. F. Page, in E. A. Almond, C. A. Brookes and R. Warren (eds.), *Proc. 2nd Int. Conf. on the Science of Hard Materials, Rhodes, September 23–28, 1984*, in *Inst. Phys. Conf. Ser.*, *75* (1986) 789.
13 S. A. Dillich and I. L. Singer, *Proc. Int. Conf. on Surface Modifications and Coatings*, 1985, American Society for Metals, Metals Park, OH, in the press.

Materials Science and Engineering, 90 (1987) 333–338

Effects of Titanium Implantation on Cavitation Erosion of Cobalt-based Metal–Carbide Systems*

N. V. H. GATELY and S. A. DILLICH

Worcester Polytechnic Institute, Worcester, MA 01609 (U.S.A.)

(Received July 10, 1986)

ABSTRACT

Cavitation erosion tests were performed on unimplanted and titanium-implanted samples of a cobalt-based superalloy and a 6wt.%Co–WC carbide. Erosion of unimplanted superalloy samples began with crack propagation through the carbides and debonding at the carbide–matrix interfaces, after which material loss from both matrix and carbide phases took place. Implantation of the alloy resulted in diminished carbide–matrix debonding and matrix phase erosion. Consequently, the erosion resistance of the alloy was significantly increased by implantation, as shown by comparison of cumulative mass loss data for unimplanted and implanted samples. Implantation also produced an improvement in the erosion resistance of the cemented carbide material, again because of increased durability of the matrix phase.

1. INTRODUCTION

Cavitation erosion is material loss of a solid surface in a fluid due to the repeated growth and collapse of bubbles near the surface. This type of wear is a severe problem in many common engineering systems, *e.g.* hydraulic turbines and pumps, pipes and valves, mining drills, diesel engine cylinders, steam turbine blades and ship propellers. Cobalt-based superalloys, consisting of hard chromium and tungsten carbides (primarily M_7C_3 and M_6C) in softer more ductile cobalt-rich solid solutions, are among the most erosion-resistant materials commercially available [1–4]. However, the high cost of these materials as well as the uncertainties in the cobalt market are incentives for further study and, if possible, improvement of the erosion resistance of these alloys.

In a previous study, high fluence titanium implantation of a cobalt-based superalloy (Stoody 3; Co–31wt.%Cr–12.5wt.%W–2.2wt.%C; Rockwell C hardness, 54–58 HRC) was found to produce significant improvements in the tribological behavior of the alloy, as shown by dry sliding friction measurements and abrasive wear tests [5, 6]. However, these tests yielded little information on the wear mechanisms active in the alloy, other than that they can be altered by ion implantation. In this work, cavitation erosion tests were performed on unimplanted and implanted Stoody 3 samples in order to investigate further the wear modes in metal–carbide composite alloys and the manner in which they are influenced by implantation. Of particular interest were the specific contributions of the different matrix and carbide phases to the erosion of the alloy.

Cavitation erosion tests were also performed on another technologically important class of metal–carbide composites: 6wt.%-Co–WC cemented carbides (WC grain size, $\frac{1}{2}$–3 μm; Rockwell C hardness, 78 HRC).

2. EXPERIMENTAL PROCEDURE

Cavitation erosion test equipment (vibrating horn configuration) was assembled and calibrated according to ref. 4. A schematic diagram of the test apparatus can be seen in Fig. 1. Tests were performed under standard test conditions (frequency, 20 kHz; peak-to-peak amplitude displacement of the vibrating tip, 0.05 mm). The test liquid, distilled water, was

*Paper presented at the International Conference on Surface Modification of Metals by Ion Beams, Kingston, Canada, July 7–11, 1986.

0025-5416/87/$3.50

Elsevier Sequoia/Printed in The Netherlands

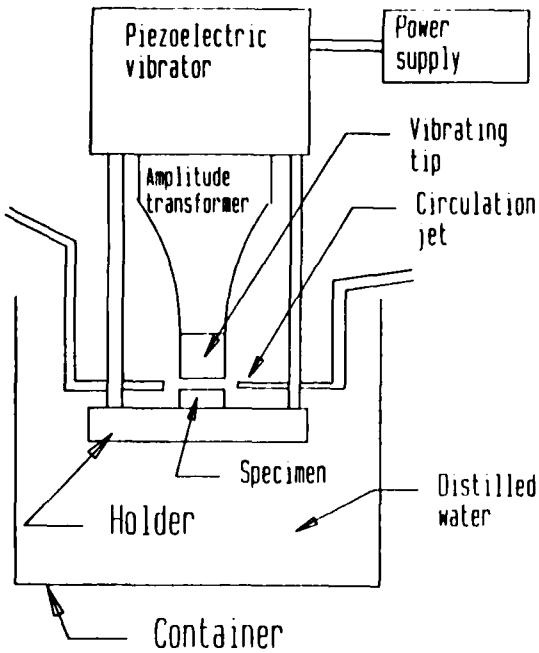

Fig. 1. Apparatus for cavitation erosion testing. The test sample is held stationary below a horn oscillating at 20 kHz with an amplitude of 0.051 mm. Air bubbles nucleated in the test liquid below the vibrating horn tip collapse on the sample surface, causing surface damage and material loss.

kept at 20 ± 2 °C by means of a cooling coil immersed in the test beaker. Additional cooling of the test surfaces was provided by water jets (pump circulated test water) through the sample-vibrating tip gap (Fig. 1).

Test conditions deviated from the standard in one respect: because of the extreme hardness and non-machinability of the alloy, samples were not attached to the horn by means of a threaded end. Rather, test samples were held stationary below the vibrating horn, at a stationary tip-sample separation distance of 0.5 mm. In addition to being convenient, this configuration also avoided the disadvantages of the moving sample geometry, *e.g.* stress imposed by the longitudinal vibrations of the horn even in the absence of cavitation [7] and rimming (non-uniform erosion of the sample due to an undamaged annular region around the perimeter of the sample).

Test samples were Stoody 3 disks (1.27 cm in diameter and 0.6 cm thick) and 6wt.%Co WC flats (1.27 cm square and 0.48 cm thick). Before testing, the sample surfaces were diamond polished to a 1 μm diamond finish and cleaned with organic solvents. Titanium implantations were made to a fluence of 5×10^{17} Ti^+ cm^{-2} at 190 keV.

The losses in mass of the samples due to cavitation erosion were monitored during testing by periodic determination of the mass of the samples. Erosion depths of the samples were calculated using the mass loss measurements, bulk densities (8.63 g cm^{-3} and 14.9 g cm^{-3} for the Stoody 3 alloy and the 6wt.%-Co-WC carbide respectively) and surface areas of the samples. Mass loss measurements for the Stoody 3 samples were made with a digital scale readable to 0.01 mg. A scale accurate to ±0.1 mg proved sufficient to measure the mass loss of the carbide samples. Periodic scanning electron microscopy (SEM) inspection of the samples was made during testing to monitor the initiation and progression of damage to the surfaces.

The total test time per sample varied between 15 and 35 h. Except when noted, tests were interrupted every 1-3 h for intervals of at least 5 min, to allow the surface temperatures of the samples to equilibrate.

3. RESULTS

Cumulative erosion depths of unimplanted and implanted Stoody 3 samples, run to total test times of between 20 and 35 h, are shown in Fig. 2. SEM micrographs showing the damage to one region of unimplanted sample 4 after testing for 3, 10 and 20 h can be seen in Fig. 3. A similar series of micrographs for implanted sample 3 is shown in Fig. 4. A comparison of the surfaces of these samples after testing for 20 h is provided in Fig. 5.

The incubation period (the test time before mass loss was observed) was between 5 and 10 h for the unimplanted samples. Increases in the rates of erosion (*i.e.* increases in the cumulative depth of erosion per unit time) were noticed after 20 h for samples 2 and 4, and again after 25 h for sample 2 (the break in the ordinate axis should be noted). As was mentioned previously, samples were interrupted during testing at intervals of the order of an hour. Unimplanted sample 1 was an exception in that it was tested for 20 h without interruption before determination of its mass. Also, titanium-implanted sample 2 was tested without interruption between 5 and 15

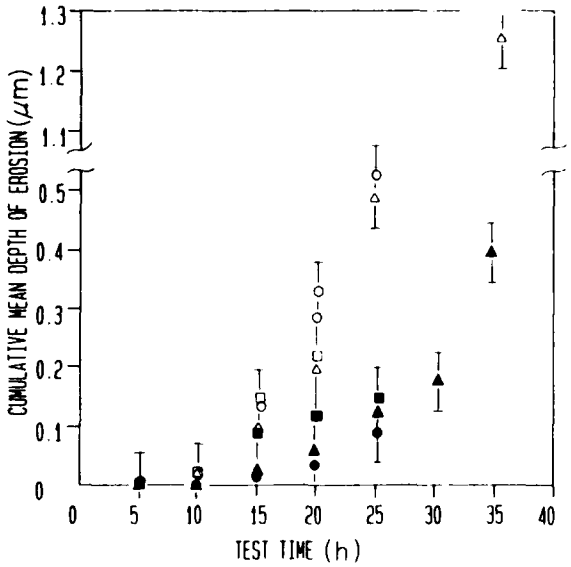

Fig. 2. Mean depth of erosion in micrometers (10^{-6} m) *vs.* test time for unimplanted and titanium-implanted samples of Stoody 3: ○, unimplanted sample 1; △, unimplanted sample 2; □, unimplanted sample 3; ○, unimplanted sample 4; ▲, titanium-implanted sample 1; ■, titanium-implanted sample 2; ●, titanium-implanted sample 3.

h. The higher erosion rates observed for these samples during these time periods compared with the other test samples suggests that the erosion rate increases with increasing length of the exposure interval, as well as with increasing cumulative exposure time.

Damage to the surfaces, namely crack propagation through the carbides and debonding at carbide-matrix interfaces (Fig. 3(a)), could be observed under SEM examination after the first hour of testing. After testing for about 5-10 h, some damage to the matrix phase could also be detected (Fig. 3(b)). Material loss from both carbides and matrix occurred after about 10 h, so that by 20 h microstructural features previously seen on the surfaces were barely recognizable (Figs. 3(c) and 5(a)).

The cumulative depths of erosion were much lower for the titanium-implanted samples (Fig. 2). The incubation period for these samples was 15 h, as opposed to less than 10 h for the unimplanted samples, after which material loss progressed steadily at erosion rates about one-third of that of the unimplanted samples. The titanium-implanted sample tested for 35 h, sample 1 (full triangle in Fig. 2), however, did show an increase in erosion rate at 30 h.

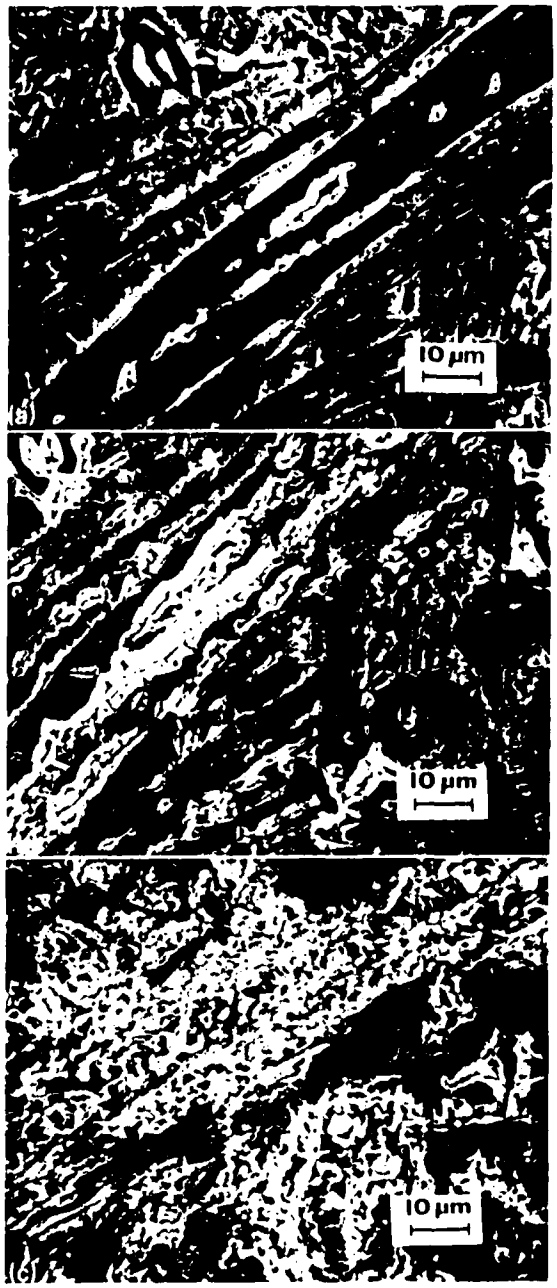

Fig. 3. SEM micrographs of a region on Stoody 3 sample 4 after testing for (a) 3 h, (b) 10 h and (c) 20 h.

As in the unimplanted sample tests, surface damage began with crack nucleation and propagation through the larger carbides (Fig. 4(a)). Initial material loss occurred primarily from carbide crack sites (Figs. 4(b), 4(c) and 5(b)). Cohesion at the carbide-matrix interfaces appeared to be enhanced relative to that in the unimplanted samples, although some

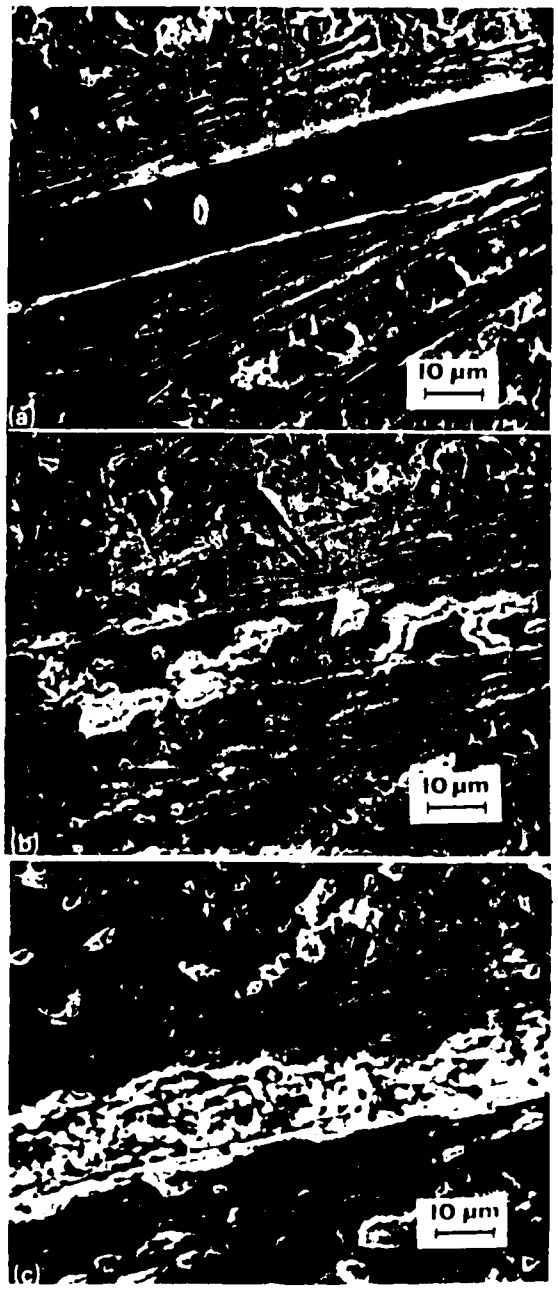

Fig. 4. SEM micrographs of a region on Stoody 3 titanium-implanted sample 3 after testing for (a) 3 h, (b) 10 h and (c) 20 h.

debonding at these interfaces was again observed. Only after testing for about 15 h was material loss from the matrix phase observed, and then to a lesser extent than in the unimplanted samples (compare Figs. 3(c) and 4(c) and Figs. 5(a) and 5(b)). However, as was the case for unimplanted samples, surface damage

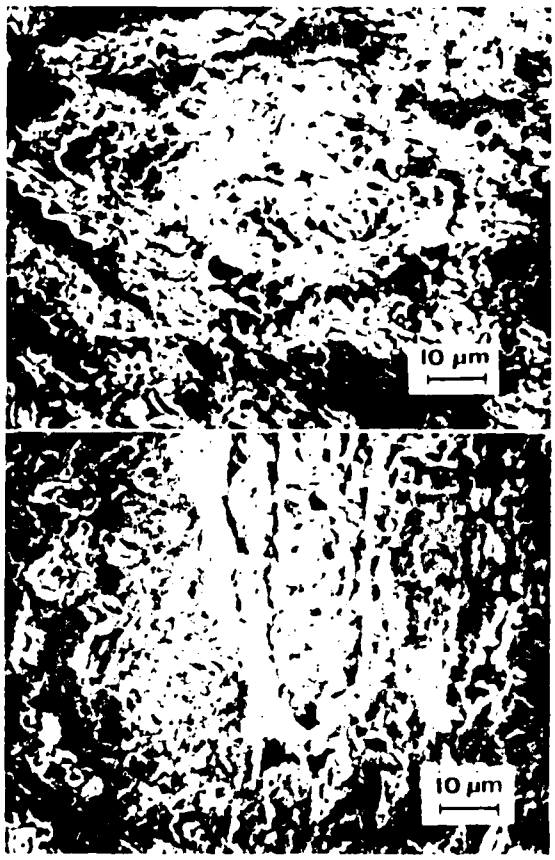

Fig. 5. SEM micrographs of (a) an unimplanted sample and (b) an implanted sample of Stoody 3 after testing for 20 h. Severe damage occurred to both matrix and carbide phases on the unimplanted sample. Less damage to the matrix phase was observed on the implanted sample.

progressed rapidly after the appearance of matrix phase erosion.

The cumulative depths of erosion of the unimplanted and implanted 6wt.%Co WC samples are shown in Fig. 6. The incubation periods for these samples were less than 1 h. Not only did material loss begin earlier in the carbide samples than in the Stoody alloy, but also it progressed at a rate which was an order of magnitude higher (compare Figs. 2 and 6). Erosion initiated at voids originally present on the surfaces. After testing for 5 h, little of the cobalt binder phase remained on the carbide surfaces which, as shown by SEM and energy dispersive X ray examinations, consisted almost entirely of WC particles (Fig. 7(a)).

The implanted carbide sample showed an erosion rate about 50% lower than that of the

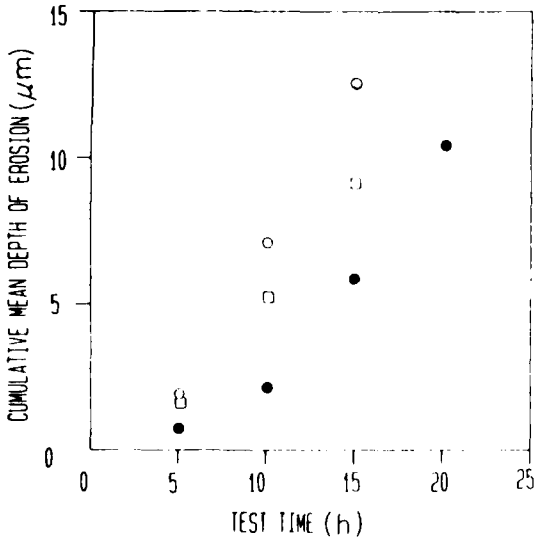

Fig. 6. Mean depth of erosion in micrometers (10^{-6} m) *vs.* test time for unimplanted and titanium-implanted samples of a 6wt.%Co-WC carbide: ○, unimplanted sample 1; □, unimplanted sample 2; ●, titanium-implanted sample.

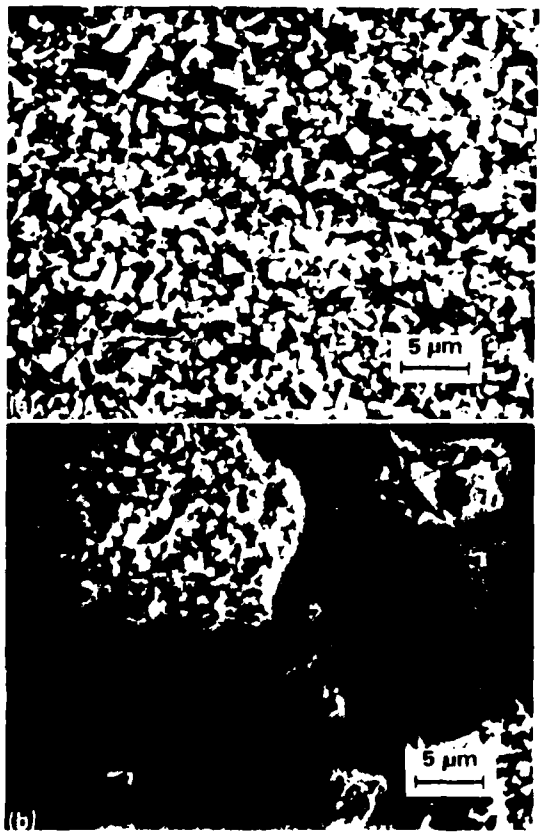

Fig. 7. SEM micrographs of (a) an unimplanted sample and (b) a titanium-implanted sample of 6wt.%Co-WC after testing for 5 h.

unimplanted samples (Fig. 6). Again, surface voids acted as erosion initiation sites. In this case, however, the cobalt binder phase was removed more slowly. As Fig. 7(b) shows, much of the original surface remained intact after testing for 5 h. By 15 h, the surface binder phase material had been almost entirely removed from the implanted sample, and there was no longer any distinguishable difference between the appearance of this surface and that of the unimplanted samples.

4. DISCUSSION

The results described above indicate that under high impact stress conditions, such as are encountered during cavitation, the wear resistance of the Stoody 3 alloy is determined by the endurance of the cobalt-based matrix phase. Erosion of this phase is preceded by debonding of the matrix from the larger of the carbides, presumably because of differences between the elastic moduli and plasticities of the phases [8]. Although material loss from the second-phase carbides was observed on both unimplanted and implanted Stoody 3 samples, measurable sample mass loss coincided with the appearance of damage to the matrix phase.

Material loss and damage to the carbides on implanted Stoody 3 surfaces appeared, under SEM examination, comparable with or perhaps slightly less than that on the unimplanted samples. Carbide–matrix debonding and matrix phase erosion were inhibited on the implanted samples, yielding a longer incubation period and lower erosion rates relative to the unimplanted samples.

Significantly lower cumulative depths of erosion for implanted surfaces, relative to those of unimplanted surfaces, may persist long after the loss of the implant layer, as is suggested by the data for implanted sample 1 (full triangle in Fig. 2). As was previously described, an increase in the erosion rate of this sample was observed after testing for 30 h and a mean depth of erosion of 0.17 μm, *i.e.* approximately the depth of the original implant layer [5]. Since the erosion rates of the unimplanted samples were not constant but rather increased with time, the cumulative depth of erosion of the implanted sample at 35 h was still only one-third of that of the

corresponding unimplanted sample (open triangle in Fig. 2). It can be expected therefore that, despite the removal of the implant layer, the ratio of the cumulative wear loss of initially implanted samples to that of unimplanted samples will increase only slowly with extended exposure to cavitation.

The superior erosion resistance of the titanium-implanted Stoody 3 samples is consistent with chemical and microstructural changes observed in the alloy after implantation. High fluence titanium implantation of the Stoody alloy has been found to produce a carburized surface layer [5] with an amorphous matrix phase and recrystallized carbides [9]. A corresponding toughening of the matrix phase and softening of the carbides can account for the observed increased erosion resistance of the matrix and enhanced carbide-matrix cohesion.

The 6wt.%Co-WC samples eroded much more quickly than did the Stoody 3 alloy samples, a consequence, most likely, of the higher porosity and carbide-metal interface density of these samples. Debonding at the carbide-metal interfaces and the subsequent rapid loss of the cobalt binder phase resulted in attrition rather than erosion of the carbide particles.

A lower erosion rate, together with increased erosion resistance of the binder phase, was observed for the implanted carbide sample. Structural changes in this material due to implantation have not been determined. However, it seems probable that, as was the case for the Stoody alloy, toughening of the cobalt binder and enhanced carbide-metal cohesion were the results of implantation-induced amorphization of the binder phase.

5. SUMMARY

Cavitation erosion testing provided a high impact stress non-contact accelerated wear situation by which the wear resistance contributions of separate components of multiphase alloys and carbides, as well as the changes produced by implantation, could be evaluated. In both materials tested, a cobalt-based superalloy (Stoody 3) and 6wt.%Co-WC, resistance to erosive wear was controlled by the durability of the matrix phase. Titanium implantation improved the erosion resistance of both materials as a result of implantation-enhanced cohesion at carbide-metal interfaces and toughening of the cobalt-based matrix and binder phases.

ACKNOWLEDGMENTS

We thank the GTE Research Laboratories in Waltham, MA, for the donation of the cemented carbide samples and the Surface Modification and Materials Analysis Group at the Naval Research Laboratory for the sample implantations.

This work was supported by the Office of Naval Research.

REFERENCES

1 K. C. Antony, *J. Met.*, *25* (1973) 52.
2 K. J. Bhansali and A. E. Miller, *Wear*, *75* (1982) 241–252.
3 C. J. Heathcock, A. Ball and B. E. Protheroe, *Wear*, *71* (1981–1982) 254–258.
4 *ASTM Stand. G 32-85*, in *ASTM Standards*, Vol. 03.02, ASTM, Philadelphia, PA, 1985, pp. 187–194.
5 S. A. Dillich and I. L. Singer, *Thin Solid Films*, *73* (1981) 219–227.
6 S. A. Dillich, R. N. Bolster and I. L. Singer, in G. K. Hubler, O. W. Holland, C. R. Clayton and C. W. White (eds.), *Ion Implantation and Ion Beam Processing of Materials. Materials Research Society Symp. Proc., Boston, MA, November 14–17, 1983*, Vol. 27, Elsevier, New York, 1984, pp. 661–666.
7 C. M. Preece, *Cavitation Erosion, Treatise Mater. Sci. Technol.*, *16* (1979) 249–308.
8 C. J. Heathcock, B. E. Protheroe and A. Ball, *Wear*, *81* (1982) 311–327.
9 S. A. Dillich and R. R. Biederman, *Proc. Int. Conf. on Surface Modification of Metals by Ion Beams, Kingston, July 7–11, 1986*, in *Mater. Sci. Eng.*, *90* (1987).

X-RAY DIFFRACTION EVALUATION OF THE EFFECTS OF NITROGEN IMPLANTATION ON STRESS INDUCED STRUCTURAL CHANGES IN A COBALT BASED ALLOY

N. V. H. Gately and S. A. Dillich

Presented at the 20th Annual Convention of the International Metallographic Society, July 27-30, 1987, Monterey, California.
To be published in V. 16 of Microstructural Science.

X-RAY DIFFRACTION EVALUATION OF THE EFFECTS OF NITROGEN IMPLANTATION ON STRESS INDUCED STRUCTRUAL CHANGES IN A COBALT BASED ALLOY

N. V. H. Gately* and S. A. Dillich**

ABSTRACT

X-ray diffraction with a GE XRD5 diffractometer, as well as glancing angle diffraction with a Read thin film camera, were used to investigate the effects of high fluence N implantation on microstructural changes in a cobalt based superalloy during wear. Nonimplanted and N implanted alloy surfaces were examined before and after cavitation erosion tests. The surface hcp/fcc ratio for the cobalt rich matrix phase of the alloy increased with erosion time for both nonimplanted and implanted samples, but to a lesser extent in the implanted samples. The differences in abrasion, erosion and galling wear resistances observed between nonimplanted and N implanted alloy samples can be explained by the suppression of stress induced fcc-hcp transformations, i.e retention of the fcc phase, within the implant layer of implanted surfaces.

* General Machinery Company, Div. of Wheaton Industries, 1201 North Street, Millville, N.J. 08332

** Department of Mechanical Engineering, Worcester Polytechnic Institute, Worcester, Ma. 01609

INTRODUCTION

Previous investigations into the effects of high fluence N implantation on the tribology of a cobalt based superalloy (Stoody 3, Co-31wt%Cr-12.5wt%W-2.2wt%C, 54-58 HRC) revealed significant changes in the deformation modes and wear rates of the alloy during dry sliding friction [1], abrasion [1] and cavitation erosion (2). The dry sliding friction coefficients of the alloy remained high after implantation, however, the wear tracks appeared rougher, with less debris formed during sliding, than those on nonimplanted surfaces. N implantation reduced the abrasion resistance of the alloy by about 50% (Fig. 1). In contrast, the cavitation erosion resistance of the alloy improved by approximately 50% following implantation (Fig. 2). Transmission electron microscope examinations of nonimplanted and implanted alloy foils showed the alloy to consist of several morphologies of single-crystal carbides (Cr-Co-W solutions) in a cobalt-rich matrix phase [3]. This phase was fcc and contained networks of planar defects (predominantly stacking faults) in both nonimplanted and implanted foils. However, a dramatic increase in the stacking fault density, with a corresponding apparent decrease in stacking fault width was observed in N implanted foils [2,3].

Cobalt based alloys designed to have low stacking fault energy, metastable fcc matrix phases are known to undergo stress induced martensitic fcc to hcp transformations during abrasion

and erosion [4-6]. Consequently, a harder, more brittle hcp surface is continuously generated on the ductile fcc bulk alloys during wear. Compositional and/or structural changes in an alloy which inhibit these transformations, i.e. stabilize the fcc phase of the alloy, effect the wear resistance.

Scanning electron microscope examinations of cavitation eroded Stoody alloy surfaces show reduced matrix phase damage and carbide-matrix debonding on implanted eroded surfaces [2], suggesting that the tribological changes observed in the alloy following implantation are the result, primarily, of implantation effects in the matrix phase. The intent of this work was to investigate the possibility that high fluence N implantation alters the ability of this phase to transform to the hcp structure in response to surface stress. To this end, X-ray diffraction examinations were made on implanted alloy surfaces before and after cavitation erosion.

EXPERIMENTAL

Test samples were Stoody 3 disks (1.27 cm in diameter and 0.6 cm thick) polished to a 1 μm diamond finish. Implantations were made to a fluence of 4×10^{17} N/cm^2 at 50 keV, corresponding to implant conditions used in the friction, abrasion, and erosion studies discussed above. Implantations were performed in a modified model 200-20A2F Varian-Extrion ion implanter with a hot-cathode arc discharge ion source. Samples

were mounted on a water cooled holder during implantation so that bulk temperatures never exceeded ~ 50^{0}C. Two pairs of nonimplanted and N implanted samples were cavitation eroded to cumulative erosion times of 3 and 10 hours, respectively. A vibrating horm apparatus was used under standard test conditions (20 KHz frequency, 0.05 mm peak to peak amplitude displacement of the vibrating tip, in distilled water at 22$\pm$2 C). Test equipment, geometry and procedure have been described in detail elsewhere [7].

X-ray diffraction examinations of the test surfaces were made, using a computer interfaced GE XRD5 diffractometer with CuK_{α} radiation, before and after periodic intervals of cavitation erosion. Peak intensity maxima (in counts/sec) were determined by Gaussian analysis of the data. Many of the fcc cobalt peaks are nearly coincident with those of the hcp cobalt phase. However, the (101) hcp peak (100% maximum intensity) and the (200) fcc peak (40% maximum intensity) are easily distinguishable. The ratio of intensities of these peaks ($I(rel)=I(101)_{hcp}/I(200)_{fcc}$) in the X-ray diffraction spectrum served as a qualitative measure of the relative amounts of the hcp and fcc phases in the alloy [4].

Calculations based on the mass adsorbtion coefficient for CuK radiation in cobalt and the density of cobalt indicated that 90% of the diffracted signals for the peaks of interest originated

from a depth ≤ 1.4 μm [8]. Implant depths at high fluence implantation are typically only 0.2-0.3 μm, consequently the majority of the X-ray information from the implanted surfaces was characteristic of the underlying nonimplanted material. In order to more closely examine the implant layer, glancing angle diffraction with a Read camera [9,10] was perfomed on a third N implanted surface, before and after cavitation erosion for 1/2 hour. XRD patterns from the Read camera were obtained using CuK_α radiation impinging on the sample surface at angles of either 5.7^0 and 20^0, corresponding to 90% sampling depths (as calculated above) of 0.4 and 1.3 μm, respectively.

RESULTS

Table 1 shows the relative intensity values, I(rel), measured on the nonimplanted and N implanted test samples as a function of cumulative erosion time. The predominantly fcc matrix alloy was found to contain a small amount of hcp phase, as indicated by the (101) hcp peak in the diffraction patterns. I(rel) i.e., the amount of hcp phase, increased with erosion time in all four surfaces examined. The implanted samples, however, showed lower rates of increase in the hcp/fcc ratio with increasing erosion time than did the nonimplanted samples, particularly after the first hour of testing. I(rel) for N implanted sample #1, tested to 10 hours, was less than half that for nonimplanted sample #1.

The data in Table 1 provide evidence that N implantation does, in fact, suppress the fcc-hcp transformations in the alloy. However the degree to which this occurs is not indicated. That is, the increase in I(rel) observed for the eroded implanted surfaces may have been the result of sub-implant layer hcp phase formation only, or of transformations within both the implant layer and the bulk material. The latter case appears most probable in light of the Read camera spectra taken on the third N implanted sample (Fig. 3). Polycrystalline ring patterns from the noneroded surface (Figs. 7a & 7b) did not contain well defined hcp phase rings. In contrast, the (101) hcp ring was clearly visible on both the 5.7^0 incidence angle (lower penetration depth) and the 20^0 incidence angle patterns taken after erosion (Figs. 7c&d), suggesting that the allotropic transformations were only partially suppressed within the implant layer.

DISCUSSION

The results described above, i.e., a lower rates of hcp phase formation on N implanted wear surfaces, are consistent with those of the TEM and tribolgy studies discussed in a previous section. Apparently, the microstructural changes in the matrix phase produced by N implantation (specifically, the increased stacking fault density and decreased fault width) improved the alloy's ability to respond plastically to an applied stress by

dislocation cross slip, rather than by martensitic shear transformations. N implanted surfaces retain a higher percentage of the softer, more ductile, fcc phase during wear than do nonimplanted surfaces. Consequently, a lower incidence of brittle fracture i.e., debris formation, but high galling deformation, was observed on the dry sliding wear tracks of implanted surfaces.

As might be predicted for surfaces with reduced transformation hardening capabilities, the abrasion resistance of the alloy decreased with implantation. The cavitation erosion resistance, on the other hand, improved with N implantation. Surfaces erode by mechanisms similar to surface fatigue [11] when exposed to high impact stress, high cycle cavitation. Under these conditions, prolonged surface ductility due to partial retention of the ductile fcc phase within the implant layer proved beneficial to the wear resistance of the alloy matrix. In addition, it seems likely that a corresponding reduction in the volume contractions which accompany the fcc to hcp transformations [12] contributed to the erosion resistance of the alloy by enhancing carbide-matrix cohesion.

CONCLUSIONS

High influence N implantation of the Stoody 3 alloy stabilizes the metastable fcc cobalt matrix phase of the alloy against martensitic fcc-hcp transformations. As a result of

the reduced incidence of these transformations during wear, implanted surfaces retain the softer, more ductile fcc phase longer than do nonimplanted surfaces. This has deleterious effects on the galling and abrasion resistance of the alloy, but improves the alloy cavitation erosion resistance.

ACKNOWLEDGEMENTS

This work was supported through the Materials Division of the Office of Naval Research. We thank the Surface Modification and Materials Analysis Group at the Naval Research Laboratory for N implantation of the alloy samples.

REFERENCES

1. S. A. Dillich, R. N. Bolster and I. L. Singer, "Friction and Wear Behavior of a Cobalt-Based Alloy Implanted with Ti or N," Ion Implantation and Ion Beam Processing of Materials, Materials Research Society Symposia Proceedings, Vol. 27, Elsevier, New York, pp. 637-642 (1984).

2. N. V. H. Gately and S. A. Dillich, "Effects of N Implantation on the Tribology and Microstructure of Cobalt Based Systems", submitted for publication, (1987).

3. S. A. Dillich and R. R. Biederman, "Structural Changes in a Cobalt-based Alloy after High Fluence Ion Implantation", Mater. Sci. Eng., Vol. 90, pp. 91-97 (1987).

4. C. J. Heathcock, A. Ball, and B. E. Protheroe, "Cavitation Erosion of Cobalt-Based Stellite Alloys, Cemented Carbides and Surface-Treated Low Alloy Steels", Wear, Vol 74, pp. 11-26 (1981-1982).

5. K. C. Antony, "Wear Resistant Cobalt-Base Alloys", J. Metals, Vol. 25, pp. 52-60 (1973).

6. K. J. Bhansali and A. E. Miller, "Role of Stacking Fault Energy on the Galling and Wear Behavior of a Cobalt Base Alloy", Wear, Vol. 75, pp. 241-252 (1982).

7. N. V. H. Gately and S. A. Dillich, "Effects of Titanium Implantation on Cavitation Erosion of Cobalt-based Metal-Carbide Systems", Mater. Sci. Eng., Vol. 90, pp. 333-338 (1987).

8. B. D. Cullity, Elements of X-Ray Diffraction, 2nd ed., Addison Wesley, Reading, Ma., pp. 292-295 (1978).

9. M. H. Read and D. H. Hensler, "X-Ray Analysis of Sputtered Films of Beta-Tantalum and Body Centered Cubic Tantalum", Thin Solid Films, Vol. 10, pp. 123-135 (1972).

10. L. C. Feldman and J. W. Mayer, Fundamentals of Surface and Thin Film Analysis, North Holland, New York, pp. 167-173 (1986).

11. C. M. Preece, ed., Treatise on Materials Science and Technology, Vol. 16, Academic Press, New York, pp. 249-308 (1979).

12. R. S. Young, ed., Cobalt, Its Chemistry, Metallurgy, and Uses, American Chemical Society Monograph Series, Reinhold, New York, p. 65 (1960).

LIST OF FIGURES

Figure 1. Relative wear resistance of N implanted Stoody 3 disks abraded with 1-5 μm diamond vs. depth (Ref. 1).

Figure 2. Average cumulative mean depths of erosion in microns (10^{-6} m) for three nonimplanted and three N implanted Stoody 3 samples. Error bars denote the standard deviation in measurements for three samples.

Figure 3. Read camera X-ray diffraction patterns from a N implanted sample (a) before cavitation erosion, 5.7^0 angle of incidence, (b) before cavitation erosion, 20^0 angle of incidence, (c) after 1/2 hour cavitation erosion, 5.7^0 angle of incidence, (d) after 1/2 hour cavitation erosion, 20^0 angle of incidence. Only half of each pattern i.e., the portion with the high intensity, low index rings, is shown. The (101) hcp ring is barely detectable in the patterns taken before cavitation erosion of the sample, but is clearly visible on both the lower and higher angle of incidence patterns after cavitation erosion.

TABLE 1. RELATIVE X-RAY DIFFRACTION PEAK INTENSITIES, I(rel), FOR NONIMPLANTED AND N IMPLANTED SAMPLE SURFACES, BEFORE AND AFTER CAVITATION EROSION TESTING ($I(rel) = I(101)_{hcp} / I(200)_{fcc}$).

CUMULATIVE EROSION TIME (HRS)	I(rel) NONIMPLANTED #1	I(rel) NONIMPLANTED #2	I(rel) N IMPLANTED #1	I(rel) N IMPLANTED #2	% INCREASE IN I(rel) NONIMPL. #1	% INCREASE IN I(rel) NONIMPL. #2	% INCREASE IN I(rel) IMPL. #1	% INCREASE IN I(rel) IMPL. #2
0	0.62	0.15	0.68	0.64	-	-	-	-
0.5	0.98	0.53	0.86	0.92	58	253	26	44
1	1.81	1.15	1.12	1.11	192	667	65	73
2	3.21	1.65	1.33	1.47	418	1000	96	286
3	3.31	1.98	2.43	2.56	434	1220	257	300
5	6.34		4.07		923		499	
10	10.40		4.82		1577		609	

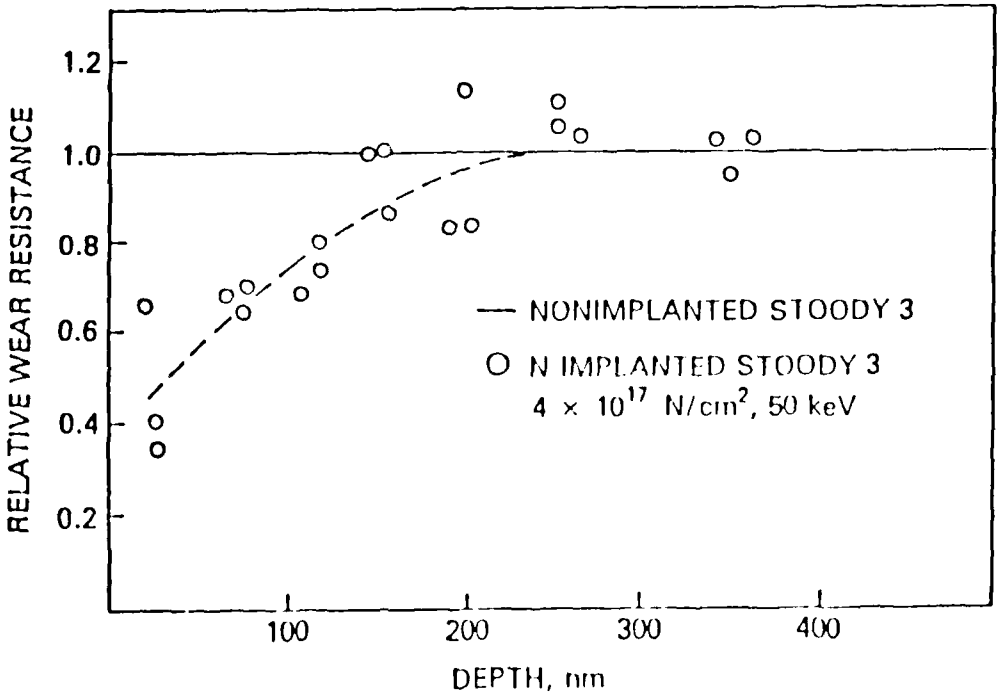
RELATIVE WEAR RESISTANCE
1.2
1.0
0.8
0.6
0.4
0.2
100
200
300
400
DEPTH, nm
— NONIMPLANTED STOODY 3
O N IMPLANTED STOODY 3
4 × 10^17 N/cm^2, 50 keV

FIGURE 1

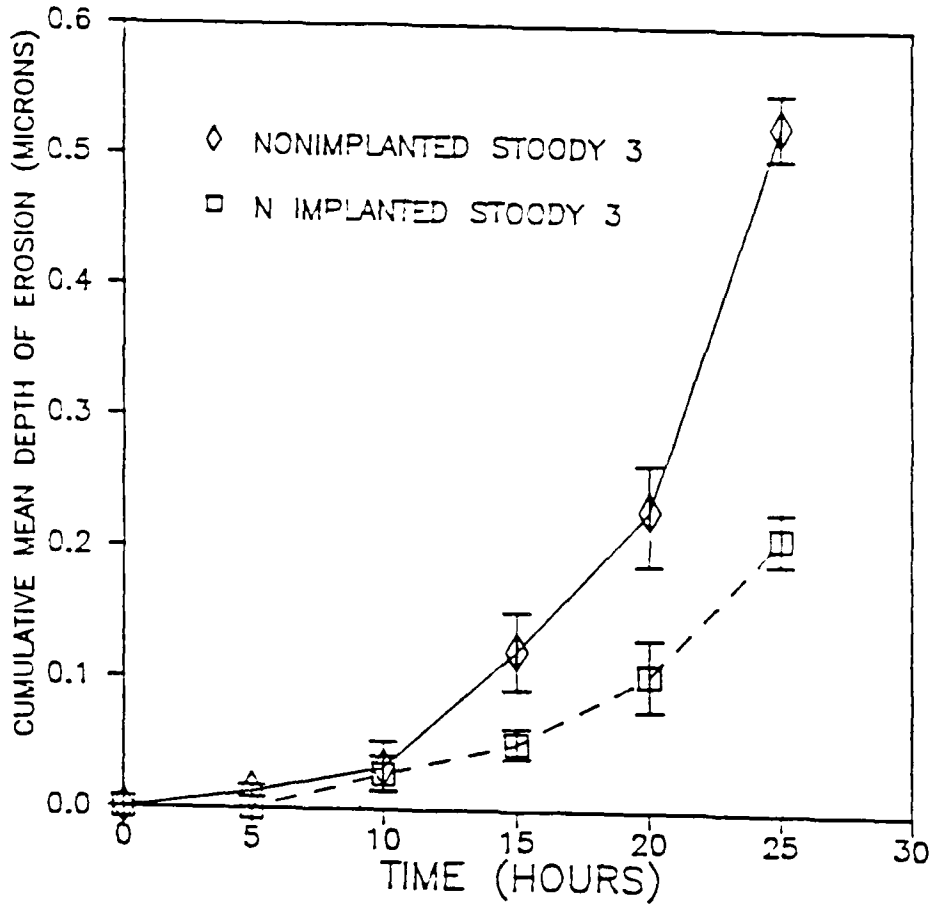
NONIMPLANTED STOODY 3
N IMPLANTED STOODY 3
CUMULATIVE MEAN DEPTH OF EROSION (MICRONS)
0.0
0.1
0.2
0.3
0.4
0.5
0.6
0
5
10
15
20
25
30
TIME (HOURS)

FIGURE 2

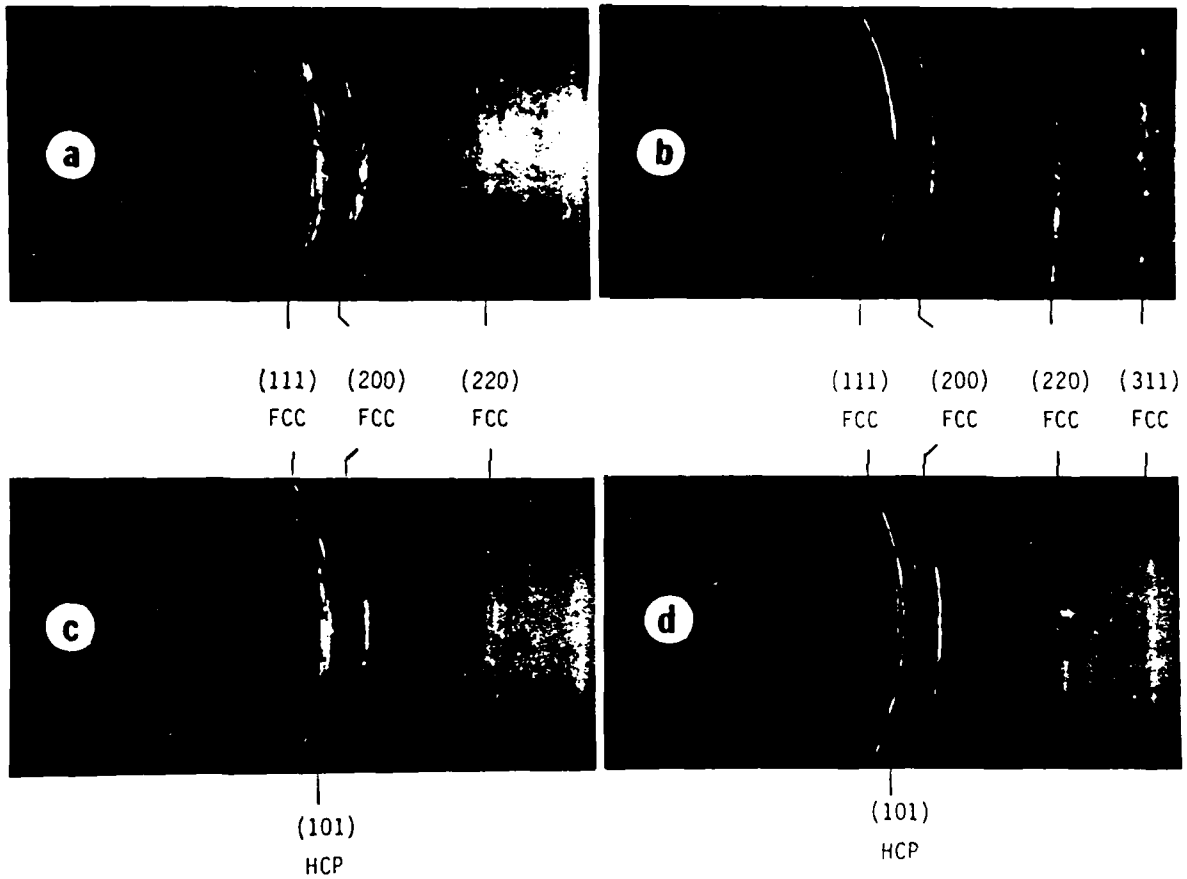

FIGURE 3. READ CAMERA X-RAY DIFFRACTION PATTERNS FROM A N-IMPLANTED SAMPLE (a) BEFORE CAVITATION EROSION, 5.7° ANGLE OF INCIDENCE, (b) BEFORE CAVITATION EROSION, 20° ANGLE OF INCIDENCE, (c) AFTER 1/2 HOUR CAVITIATION EROSION, 5.7° ANGLE OF INCIDENCE, (d) AFTER 1/2 HOUR CAVITATION EROSION, 20° ANGLE OF INCIDENCE.

EFFECTS OF N IMPLANTATION ON THE TRIBOLOGY
AND MICROSTRUCTURE OF COBALT BASED SYSTEMS

[illegible] and S. A. Dillich

[illegible] Conference on Metallurgical
[illegible] San Diego, California.

[illegible] Surface and Coatings Technology.

SUMMARY

High fluence N implantation improved the cavitation erosion resistance of a cobalt based superalloy (Stoody 3), primarily as as a result of implantation effects in the cobalt based matrix phase. As shown by X-ray diffraction examinations of eroded alloy surfaces, the metastable fcc matrix phase is stabilized by implantation. Prolonged matrix phase ductility and decreased carbide-matrix debonding were the results of the reduced incidence of stress induced fcc to hcp transformations in the implanted surfaces during cavitation. In contrast, retention of the softer, more ductile fcc phase is detrimental to the abrasive wear resistance of the alloy. The cavitation erosion resistance of a 6wt% Co-WC cemented carbide also improved with implantation, again because of increased durability of the matrix phase.

EFFECTS OF N IMPLANTATION ON THE TRIBOLOGY AND MICROSTRUCTURE OF COBALT BASED SYSTEMS

N.V.H. Gately and S.A. Dillich, Dept. of Mechanical Engineering, Worcester Polytechnic Institute, Worcester, Mass. 01609

INTRODUCTION

The effects of nitrogen implantation on properties and microstructures of cobalt based metal/carbide systems have been explored by many investigators during the past decade[1-8]. Although changes in the mechanical properties and tribological behavior of these materials have been observed, mechanisms for these changes have not been determined. In a previous work[1], dry sliding friction tests and relative abrasive wear measurements were used to investigate the effects of high fluence nitrogen implantation on the tribology of a cobalt based superalloy (Stoody 3, Co-31wt%Cr-12.5wt%W-2.2wt%C, 54-58 HRC). The relative abrasion resistance of the alloy was reduced to about one-half of the bulk value after nitrogen implantation. The dry sliding friction and surface roughening of the alloy remained high after implantation, however relatively little alloy debris was seen in the implanted wear tracks.

The superior galling and wear resistance exhibited by cobalt based alloys is often attributed to the low stacking fault energies of the metastable fcc matrix phases which allow low temperature, localized martensitic fcc to hcp transformations to occur with strain at an abraded or eroded surface[9-11].

Consequently, it is believed, the ductile fcc bulk alloys are protected by harder, more brittle hcp surfaces. Alloying additions which stabilize the fcc phase of these materials generally prove detrimental to their wear characteristics . Thus, nitrogen stabilization of the fcc matrix phase of the Stoody 3 alloy was offered as a feasible explanation of the poor abrasion resistance of the implanted surfaces[1].

In this work, cavitation erosion tests were performed on nonimplanted and N implanted samples of the Stoody alloy in order to investigate further the effects of implantation on the tribolgy of the alloy. Microstructural changes produced during wear of nonimplanted and implanted superalloy surfaces were investigated by X-ray diffraction examinations of test surfaces before and after cavitation erosion. Erosion tests were also made on another technologically important class of metal/carbide composites: 6wt%Co-WC cemented carbides (WC grain size, 1/2-3 micron, 78 HRC).

EXPERIMENTAL

Cavitation erosion material loss from a solid surface in a fluid is the result of the repeated growth and collapse of bubbles near the surface. Cavitation erosion testing, therefore, provides a noncontact (i.e. without the introduction of another surface to the system) method of investigating the high stress wear mechanisms of a material, as well as the individual

contributions of the individual phases to the wear of multiphase systems. Cavitation erosion tests were performed with a vibrating horn apparatus under standard test conditions (20 KHz frequency, 0.05 mm peak to peak amplitude displacement of the vibrating tip, in distilled water at 22±2 C). Test equipment, geometry and procedure have been described in detail elsewhere[3].

Test samples were Stoody 3 disks (1.27 cm in diameter and 0.6 cm thick) and 6 wt%Co-WC flats (1.27 cm square and 0.48 cm thick), polished before testing to a 1 micron diamond finish. Implantations were made to a fluence of 4×10^{17} N/cm^2 at 50 keV for the alloy samples, and to 4×10^{17} N/cm^2 at 90 keV for the cemented carbide samples. Alloy samples were mounted on a water cooled holder during implantation so that bulk temperatures never exceeded ~ 50^{0}C. Carbide samples, on the other hand, were not cooled during implantation in order to conform to implant conditions used by other researchers[4-6]. Bulk temperatures in these samples reached 200^{0}C or greater during implantation. Total test time per sample was either 20 or 25 hours. Tests were interrupted periodically for sample weighing and SEM surface examination. Erosion depths of the samples were calculated from the weight loss data, surface areas, and bulk densities of the samples (8.63 g-cm^{-3} and 14.9 g-cm^{-3} for the Stoody 3 alloy and the 6wt%Co-WC samples respectively).

X-ray diffraction examination of nonimplanted and N implanted Stoody surfaces were made using a GE XRD5

diffractometer with CuK_α radiation. Calculations based on the mass adsorbtion coefficient for CuK_α radiation in cobalt, and the density of cobalt indicated that 75% of the diffraction signal originated from a depth < 1 micron for small angle reflections[12] i.e., four to five times the usual implant depth at high fluences. The ratio of the intensities of the (101) hcp and the (200) fcc peaks, $I(rel)=I(101)_{hcp}/I(200)_{fcc}$, can be used as a qualitative measure of the relative amounts of the hcp and fcc phases in the alloy[10]. I(rel) was monitored as a function of cumulative erosion time from 0 to 3 hours and from 0 to 10 hours, respectively, for two pairs of nonimplanted and N implanted samples.

RESULTS

Cumulative erosion depths of nonimplanted and implanted Stoody 3 samples as a function of test time are shown in Figures 1 and 1b respectively. SEM micrographs showing the damage to one region of a nonimplanted sample after testing for 5 hours and after 20 hours are shown in Figure 2. A similar series of micrographs for the implanted samples can be seen in Figures 3 and 4.

The incubation period (elapsed test time before mass loss was observed) was between 5 and 10 hours for the nonimplanted samples. Damage to the surfaces, namely crack propagation through the carbides and debonding at carbide-matrix interfaces

(e.g, Fig. 2a) could be observed under SEM examination after the first hour of testing. Damage to the matrix phase could be detected after testing for about 5-10 hr. Material loss from both carbides and matrix occurred after about 10 hours, so that by 20 hours, microstructural features previously seen on the surfaces were barely recognizable (Fig 2b).

The as implanted surfaces appeared identical to the noninmplanted surface under SEM examination, with the exception that small blisters could occasionally be resolved on the larger carbides. N implantation also produced a noticeable change in the initial erosion mode of the alloy. Within the first 5 hours of testing, the implanted samples eroded by spalling of a thin layer first from the carbides, then from the surrounding matrix phase material (Figs. 3a and 4a). After about 10 hours this layer had been completely removed from the carbides, so that damage and material loss from these phases could be observed (Fig. 3b). As was the case for the nonimplanted samples, after 20 hours of testing, the carbides had been severely damaged, although some of the matrix phase still remained intact (Figs. 3c and 4b).

As comparison of Figs. 1a and 1b shows, the cumulative depths of erosion were significantly lower for the implanted samples. The incubation period for these samples, ~ 10 hours, was slightly longer than for the nonimplanted samples and coincided with the removal of the spalled layer from the

carbides, after which material loss progressed steadily at erosion rates about one-half that of the nonimplanted samples.

Somewhat lower erosion rates were also observed for the implanted cemented carbide samples. The cumulative depths of erosion of the noninimplanted and implanted 6w%Co-WC samples are shown in Fig. 5. The low cobalt concentration and high carbide-matrix interface density of these samples resulted in rapid loss of the cobalt binder phase from the test surfaces, incubation periods less than an hour, and high erosion rates (an order of magnitude higher than for the Stoody alloy samples). After testing for 5 hours, little of the cobalt binder phase remained on the nonimplanted cemented carbide surfaces which, as shown by SEM and energy dispersive X-ray examinations, consisted almost entirely of WC particles (Fig. 6a). Carbide particles did not appear to suffer erosive damage or material loss but, rather, fell from the surfaces as a consequence of the loss of the matrix phase. The implanted cemented carbide samples eroded in a similar manner, with the exception that the matrix phase persisted somewhat longer than on the nonimplanted samples (Fig 6b). Neither blistering nor spalling were observed on the implanted surfaces.

Results of the X-ray diffraction examinations of the nonimplanted and implanted Stoody 3 alloy surfaces are summarized in Table I. The before testing surfaces were found to be predomimantly fcc, however the presence of a small amount of hcp

phase in the alloy was indicated by the (101) hcp peak in the diffraction patterns. The amount of hcp phase increased with cumulative erosion time in all four samples examined, as shown by the I(rel) values in Table I. However, with increasing test time, the implanted samples showed consistently lower rate of increase in the hcp/fcc ratio than did the nonimplanted samples.

Microstructural features of the nonimplanted and implanted alloy have also been investigated using TEM/SAD examinations[2]. The matrix phase of the alloy contained networks of planar defects (predominantly stacking faults) running through the grains (e.g.,see Fig. 7a). A striking increase in this fault density, with a corresponding apparent decrease in stacking fault width was observed after nitrogen implantation (Fig. 7b). Single crystal diffraction patterns from the matrix phase of the foils found evidence only of the fcc matrix phase in both implanted and nonimplanted samples. The large complex carbides appeared opaque, defect free and single crystalline in both implanted and nonimplanted foils.

DISCUSSION

High dose gaseous ion implantation (i.e., $> 10^{17}$ ions/cm^2), can produce lateral surface compressive stresses and hardness changes in both ceramic and metallic systems[4-5,13-15] as a result of gas atom accomodation, radiation damage and local

volume changes in the host lattice. Surface blistering above a critical dose level may also occur in association with amorphisation and, in the case of ceramics, softening of the implant layer[14,15]. The spalling of a thin surface layer from the implanted Stoody surfaces in response to the cyclical tension and compression of the surfaces during cavitiation, confirmed the presence of significant compressive stresses in the implant layer. The early removal of the spalled layer from the carbides within the first few hours of testing indicates (a) that higher compressive stresses existed within these phases than in the matrix phase, possibly due to greater N retention in this phase; and/or (b) that the location of the maximum compressive stresses occurred at a shallower depth in the denser carbides than in the matrix phase.

Dramatic changes in the hardness of the carbides as a result of implantation is not indicated by either their erosion behavior or microstructural features as seen under TEM observation. Although some blistering was observed on the implanted Stoody 3 carbides, these phases remained single crystalline after implantation and showed no evidence of radiation damage or amorphization[2]. After removal of the spalled layer the carbides eroded much as those in the nonimplanted surfaces, with crack propagation followed by rapid material loss. Nevertheless, the erosion rates of these samples remained low.

Significant implantation hardening of the matrix phase also seems unlikely in light of the low abrasion resistance of N implanted samples. It seems then, that the lower erosion rates of the implanted alloy were the results, primarily, of other implantation effects in the cobalt rich matrix; namely, increased plasticity of this phase, and reduced debonding at carbide-matrix interfaces. The latter effect can be attributed to suppression of the allotropic fcc to hcp transformations in the matrix (discussed further below) and therefore, of the acccompanying volume contractions[16]; and to volume expansions in both matrix and carbide phases as a result of retained interstitial nitrogen.

The X-ray diffraction data in Table I showed evidence for a reduced incidence of fcc to hcp transformations in the eroded N implanted alloy surfaces. That is, the implanted surfaces, within the depth of ~ 1 micron sampled by the X-ray signal, retained a higher percentage of the softer, more ductile fcc phase during erosion than did the nonimplanted samples. A possible mechanism for the retention of the fcc phase is suggested by comparison of TEM micrographs of nonimplanted and implanted alloy foils (See Fig. 7). Although the stacking fault density in the alloy matrix phase was much larger after implantation, the stacking fault widths appeared smaller. A lower stacking fault width material is better able to deform plastically by dislocation motion and cross slip in response to an applied stress, and less likely to undergo martensitic stress

induced phase transformations.

The results of this study show that a reduced incidence in fcc to hcp transformations within a thin surface layer has a benificial effect on the erosion resistance of the Stoody 3 alloy. Prolonged matrix phase ductility and carbide-matrix interface cohesion resulted in increased wear resistance, in spite of retention of a softer phase, during high impact, high stress cavitation erosion. These factors did not enhance the low stress, low impact abrasion resistance of the alloy. Under these wear conditions surface hardness is the controlling materials property so that, predictably, N implantation and the accompanying retention of the fcc phase produced a diminished abrasion resistance. Similarly, galling deformation during dry sliding was exacerbated by N implantation. That is, the dominant wear mechanism of the alloy changed from one of brittle fracture and debris chip formation, characteristic of hcp materials, to one of plastic flow.

The erosion resistance of the cemented carbide samples was controlled by the cobalt binder phase and, as was the case for the Stoody alloy, increased erosion resistance of this phase was observed on implanted samples. Structural changes in the implanted cemented carbides used in this study were not determined. However, Dearnaley et. al. have reported fcc binder

phase stabilization[4,5] in cemented carbides implanted under similar conditions i.e., high fluence N at elevated temperatures. Most likely then, the improved cavitation erosion of the implanted cemented carbides can be credited to nitrogen stabilization of the fcc cobalt binder phase and a resultant strengthening of carbide-matrix cohesion.

CONCLUSIONS

Surface compressive stresses introduced in a cobalt based alloy (Stoody 3) during high dose N implantation result in an initial spalling of a thin layer and a slight increase in the incubation period during cavitation erosion, but have little effect on the subsequent erosion rate of the alloy.

The metastable fcc matrix phase in the alloy is stabilized by N implantation, thereby reducing the incidence of stress induced fcc to hcp martensitic transformations during wear. The increased retention of the softer, more ductile fcc phase on implanted surfaces, although detrimental to wear resistance during abrasion, reduces the cavitation erosion rate of the alloy due to prolonged matrix phase ductility and reduced debonding at carbide-matrix phase interfaces.

The improvement in binder phase erosion resistance observed for implanted cemented carbide samples suggests that a similar nitrogen stabilization of the fcc binder phase also occurs in this material.

ACKNOWLEDGMENTS

We thank the GTE Research Laboratories in Waltham, MA, for the donation and implantation of the cemented carbide samples and the Surface Modification and Materials Analysis Group at the Naval Research Laboratory for the alloy sample implantations.

This work was supported through the Materials Division of the Office of Naval Research.

REFERENCES

1 S.A. Dillich, R.N. Bolster and I.L. Singer, in G.K. Hubler, O.W. Holland, C.R. Clayton and C.W. White (eds.), Ion Implantation and Ion Beam Processing of Materials, Materials Research Society Symp. Proc., Boston, MA, November 14-17, 1983, Vol. 27, Elsevier, New York, 1984, p. 637.

2 S.A. Dillich and R.R. Biederman, Mater. Sci. Eng., 90 (1987) 91.

3 N.V.H. Gately and S.A. Dillich, Mater. Sci. Eng., 90 (1987) 333.

4 G. Dearnaley et. al., Nucl. Inst. and Meth. in Phys. Res., B 7/8 (1985) 188.

5 G. Dearnaley et. al., in H. Bildstein and H. M. Ortner (eds.), Proc. of the Eleventh Plansee Seminar, Metallwerk Plansee, Reutte, Austria (1985).

6 D.W. Oblas and V.K. Sarin, J. Vac. Sci. Technol., A 5 (2) Mar/Apr. (1987) 159.

7 J. Greggi, Jr. Scripto Met., 17 (1983) 765.

8 S. Fayeulle et. al., J. of Mats. Sci., 21 (1986) 1814.

9 K.J. Bhansali and A.E. Miller, Wear, 75 (1982) 241.

10 C.J. Heathcock, A. Ball and B. E. Protheroe, Wear, 74 (1981-82)11.

11 K. C. Antony, J. Met. 25 (Feb. 1973) 52.

12 B.D. Cullity, Elements of X-Ray Diffraction 2nd ed., Addison Wesley, Reading, MA., 1978 pp. 292-295.

13 N.E.W. Hartley, J. Vac. Sci. Technol., 12 No.1 Jan/Feb (1975) 485.

14 K.O. Legg, et.al., Nucl. Inst. and Meth. in Phys. Res., B 7/8 (1985) 535.

15 P.J. Burnett and T.F. Page, in E.A. Almond, C.A. Brookes and R. Warren (eds.), Science of Hard Materials, Inst. Phys. Conf. Ser. No. 75, Adam Hilger Ltd. Boston (1986) pp. 789-802.

16 "Cobalt, Its Chemistry, Metallurgy, and Uses", R.S. Young (ed), American Chemical Society Monograph Series, Reinhold, New York, (1960) 65.

LIST OF FIGURES

Figure 1. Cumulative mean depth of erosion in microns (10^{-6} meters) vs. test time for (a) nonimplanted and (b) N implanted samples of Stoody 3 alloy.

Figure 2. SEM micrographs of a region on nonimplanted Stoody 3 samples after testing for (a) 5 hours and (b) 20 hours.

Figure 3. SEM micrographs of a region on a Stoody 3 N implanted sample after testing for (a) 3 hours (b) 10 hours and (c) 20 hours.

Figure 4. SEM micrographs of a region on a Stoody 3 N implanted sample after testing for (a) 5 hours and (b) 25 hours.

Figure 5. Average cumulative mean depths of erosion in microns (10^{-6} meters) vs. test time for two nonimplanted and two N implanted samples of 6wt%Co-WC carbides. Error bars denote the standard deviations in the measurements.

Figure 6. SEM micrographs of (a) a nonimplanted sample and (b) a N implanted sample of a 6wt%Co-WC after testing for 5 hours.

Figure 7. Bright field micrographs of the Stoody 3 matrix phase in (a) a nonimplanted foil and in (b) a N implanted foil.

Table 1

RELATIVE X-RAY DIFFRACTION PEAK INTENSITIES, I(rel), FOR NONIMPLANTED AND N IMPLANTED SAMPLE SURFACES, BEFORE AND AFTER CAVITATION EROSION TESTING ($I(rel) = I(101)_{hcp} / I(200)_{fcc}$).

CUMULATIVE EROSION TIME (HRS)	I(rel) NONIMPLANTED #1	I(rel) NONIMPLANTED #2	I(rel) N IMPLANTED #1	I(rel) N IMPLANTED #2	% INCREASE IN I(rel) NONIMPL #1	% INCREASE IN I(rel) NONIMPL #2	% INCREASE IN I(rel) IMPL #1	% INCREASE IN I(rel) IMPL #2
0	0.62	0.15	0.68	0.64	-	-	-	-
0.5	0.98	0.53	0.86	0.92	58	253	26	44
1	1.81	1.15	1.12	1.11	192	667	65	73
2	3.21	1.65	1.33	1.47	418	1000	96	286
3	3.31	1.98	2.43	2.56	434	1220	257	300
5	6.34		4.07		923		499	
10	10.40		4.82		1577		609	

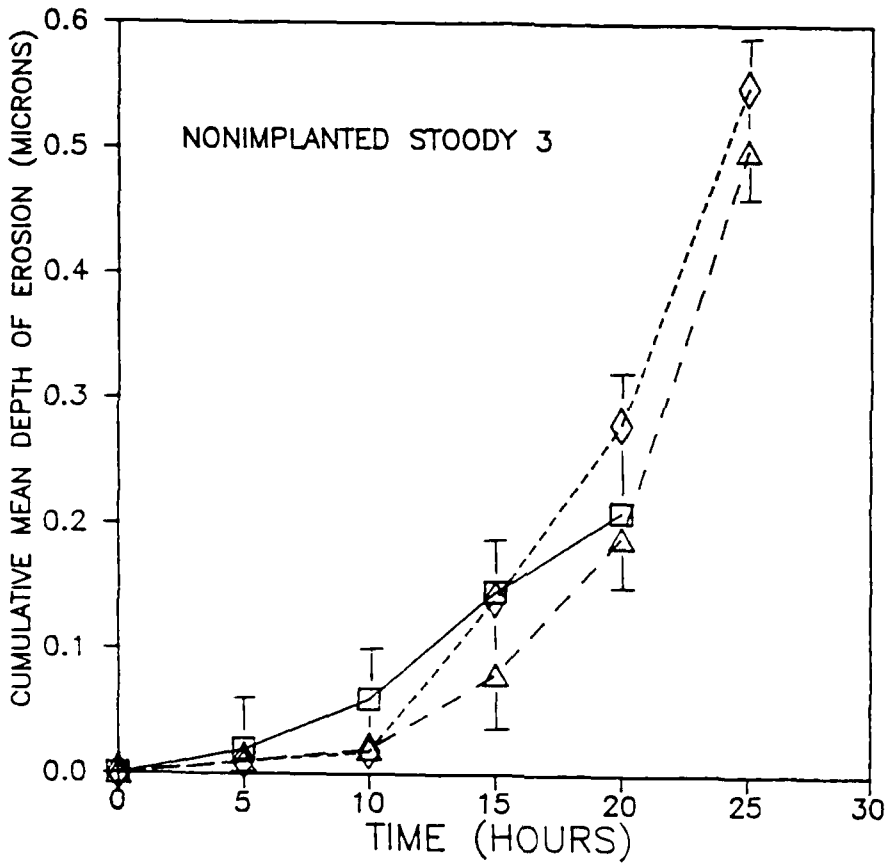
NONIMPLANTED STOODY 3
CUMULATIVE MEAN DEPTH OF EROSION (MICRONS)
0.0
0.1
0.2
0.3
0.4
0.5
0.6
0
5
10
15
20
25
30
TIME (HOURS)

FIGURE 1a

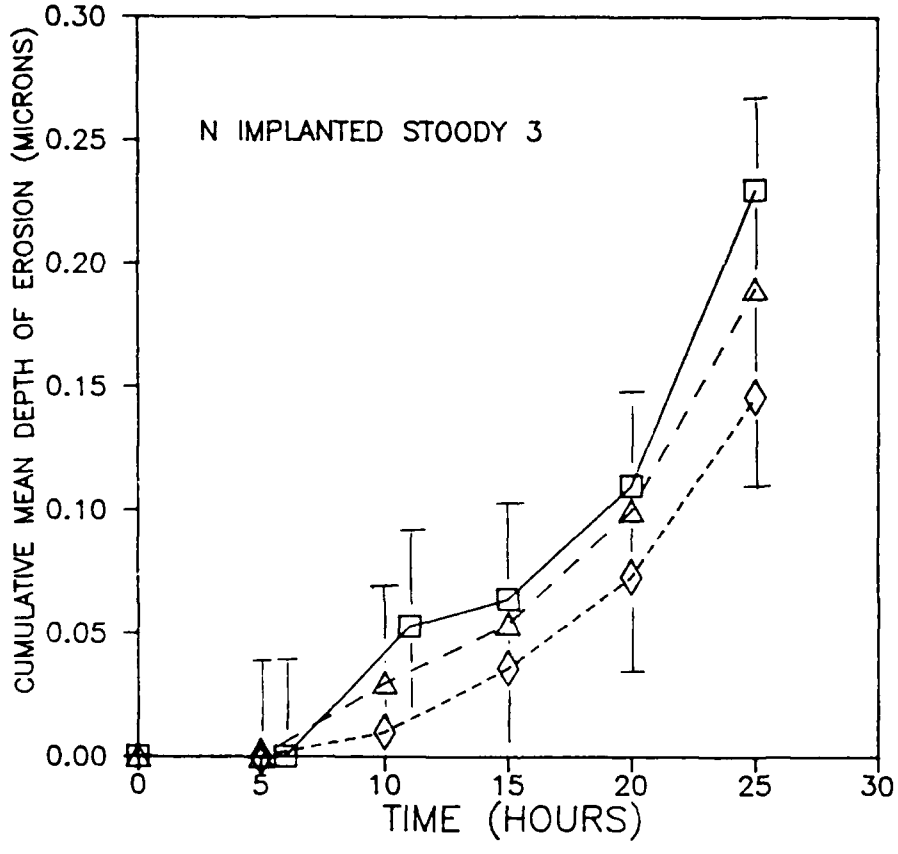
N IMPLANTED STOODY 3
CUMULATIVE MEAN DEPTH OF EROSION (MICRONS)
0.30
0.25
0.20
0.15
0.10
0.05
0.00
0
5
10
15
20
25
30
TIME (HOURS)

FIGURE 1b

(a)

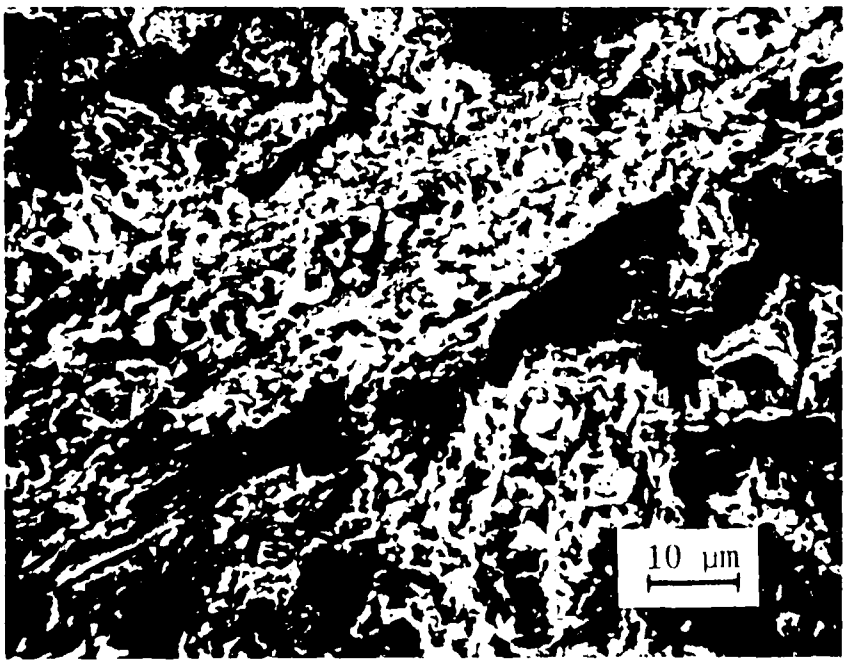

(b)

Figure 2. SEM micrographs of a region on a nonimplanted Stoody 3 sample after testing for (a) 5 hours and (b) 20 hours.

(a)

(b)

Figure 3. SEM micrographs of a region on a Stoody 3 N implanted sample after testing for (a) 3 hours and (b) 10 hours.

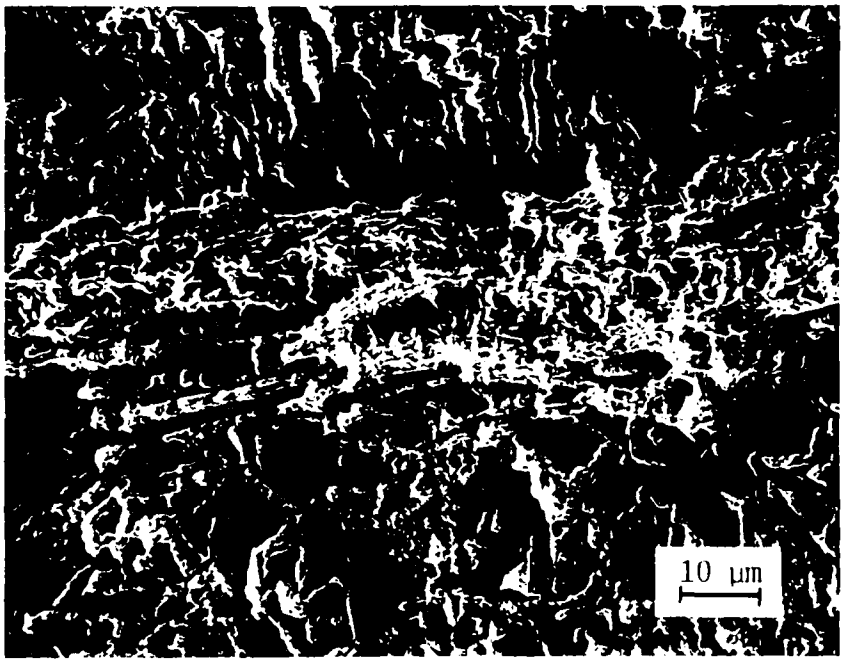

Figure 3c. SEM micrograph of a region on a Stoody 3 N implanted sample after testing for 20 hours.

(a)

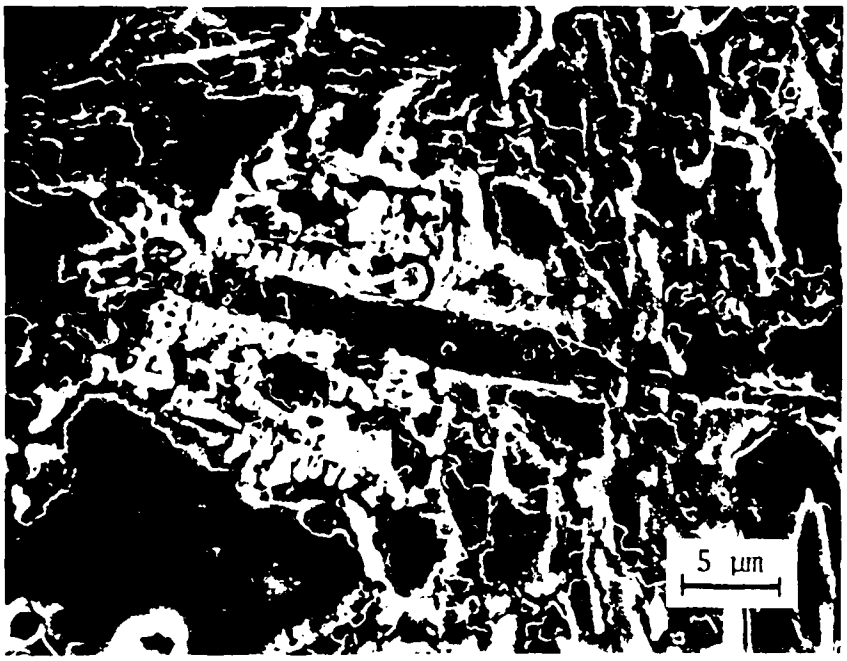

(b)

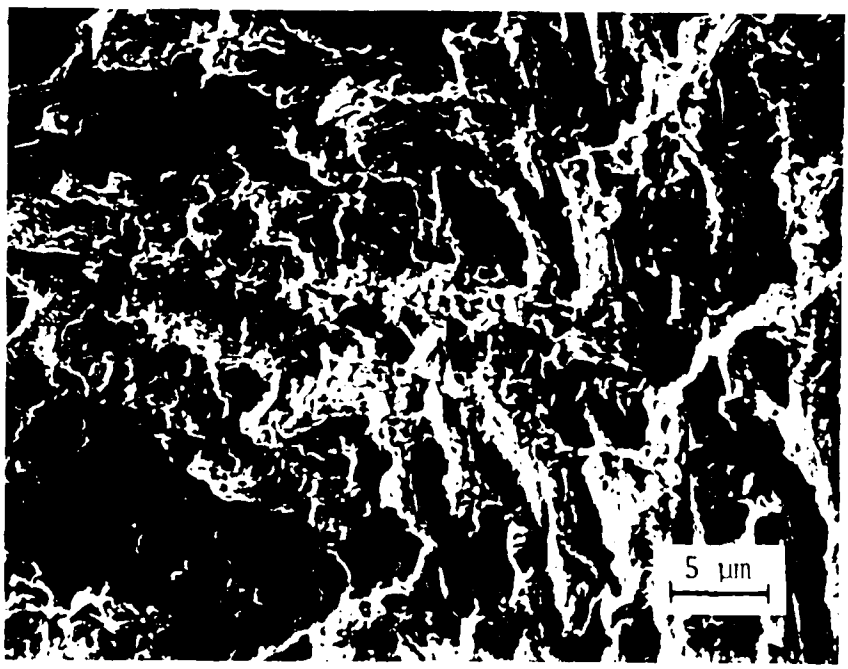

Figure 4. SEM micrographs of a region on a Steody 3 N implanted sample after testing for (a) 5 hours and (b) 25 hours.

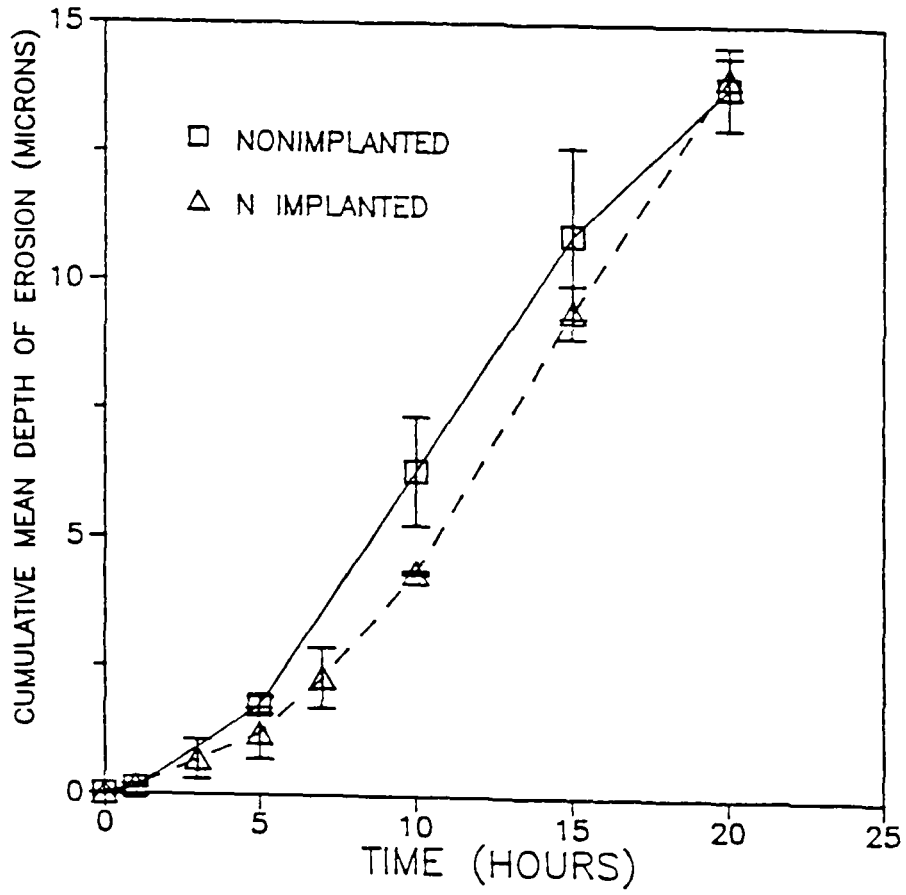
NONIMPLANTED
N IMPLANTED
CUMULATIVE MEAN DEPTH OF EROSION (MICRONS)
TIME (HOURS)
0
5
10
15
20
25

FIGURE 5

(a)

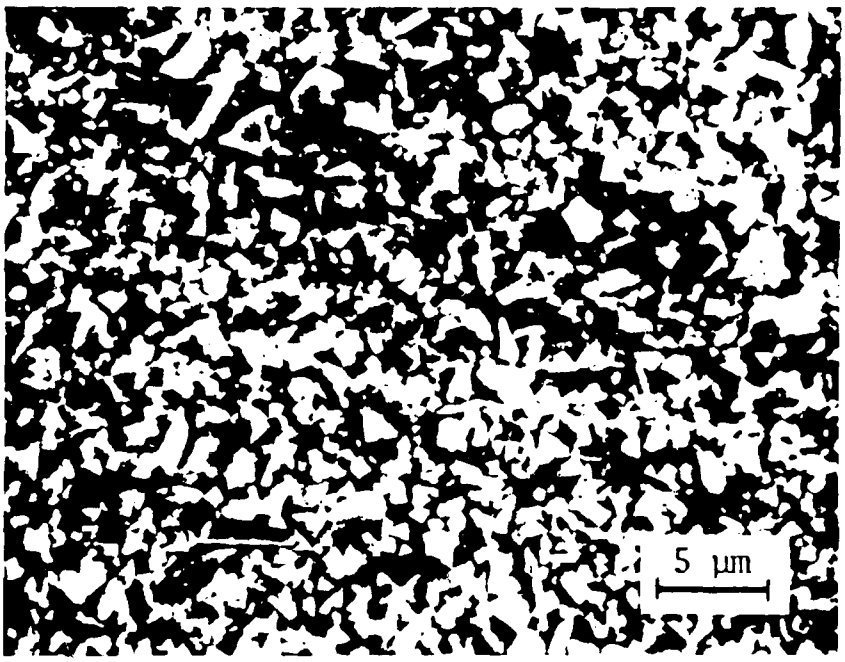

(b)

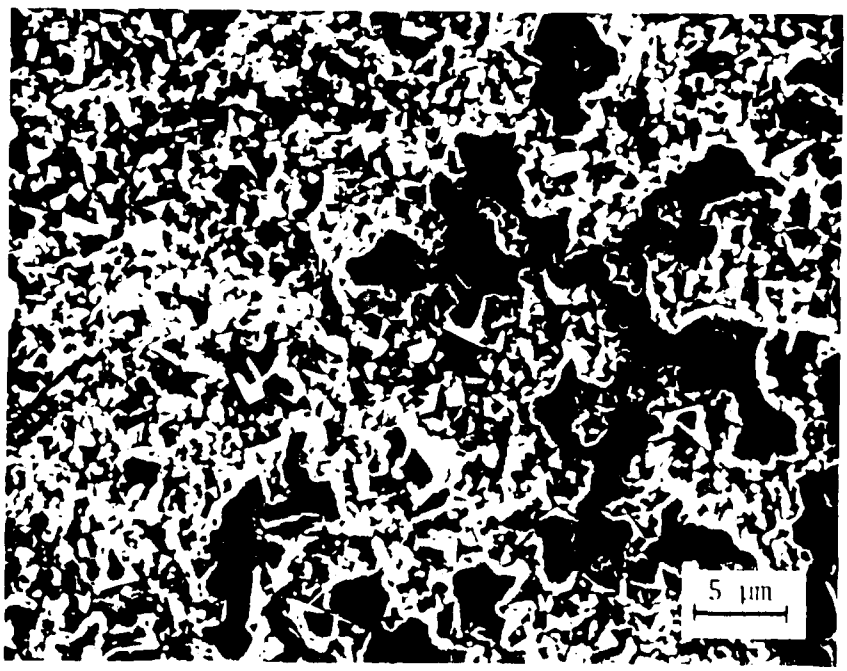

Figure 6. SEM micrographs of (a) a nonimplanted sample and (b) a N implanted sample of a 6Wt Co-WC after testing for 5 hours.

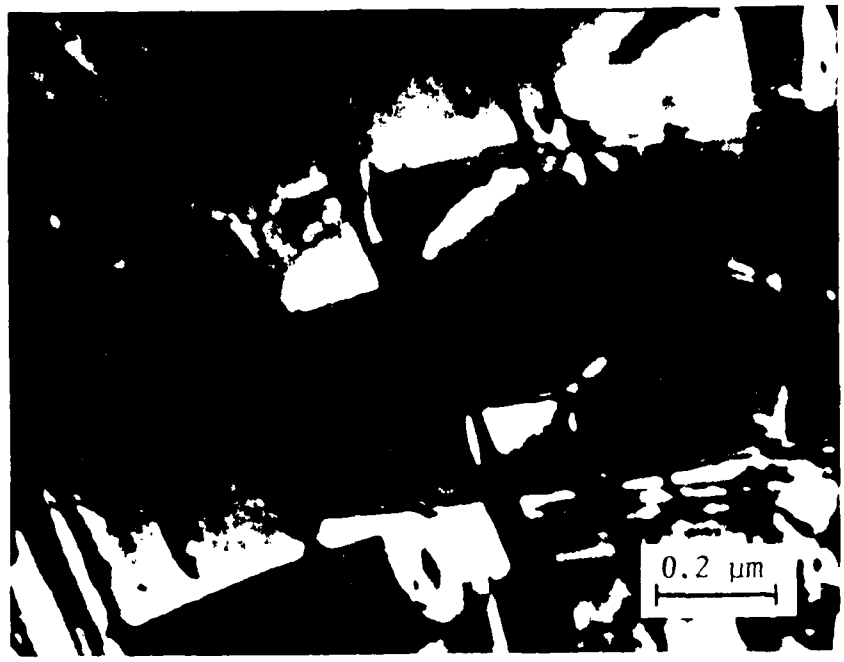

(a)

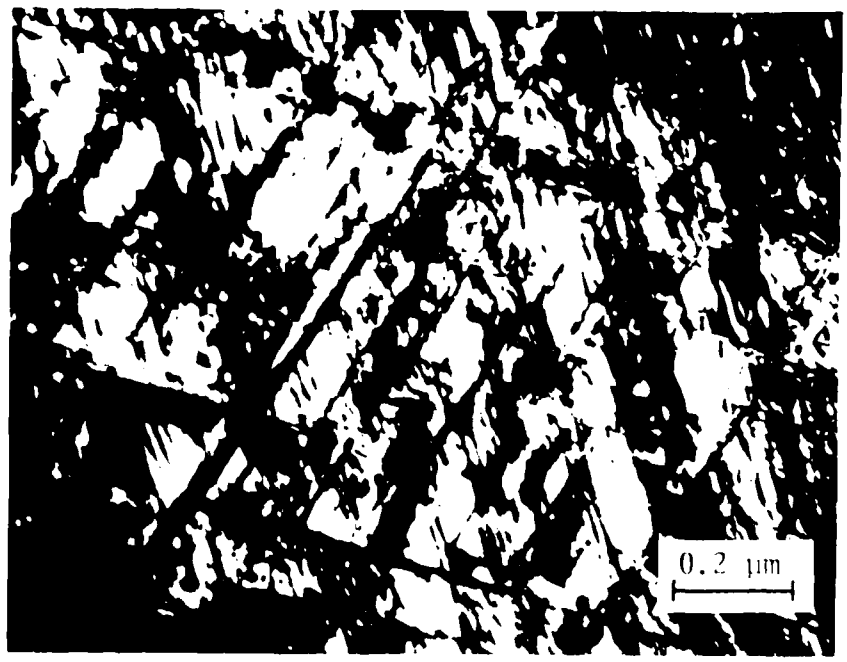

(b)

Figure 7. Bright field micrographs of the Steady 3 matrix phase in (a) a nonimplanted foil and in (b) a N implanted foil.

END
FEb.
1988
DTIC